JOURNAL OF THE AMERICAN WATER RESOURCES ASSOCIATION

AMERICAN WATER RESOURCES ASSOCIATION

Impact of Climate and Land Use Change on Streamflow and Sediment Yield in a Snow-Dominated Semiarid Mountainous Watershed

K.B. Khatri, C. Strong, N.von Stackelberg, M. Buchert, and A.K. Kochanski

Research Impact Statement: The future streamflow and sediment load in snowfed mountainous watersheds show strong sensitivity to future climate change. Sediment concentrations exhibit a nonlinear relationship with streamflow.

ABSTRACT: This study investigates the impact of climate and land use change on the magnitude and timing of streamflow and sediment yield in a snow-dominated mountainous watershed in Salt Lake County, Utah using a scenario approach and the Hydrological Simulation Program — FORTRAN model for the 2040s (year 2035–2044) and 2090s (year 2085–2094). The climate scenarios were statistically and dynamically downscaled from global climate models. Land use and land cover (LULC) changes were estimated in two ways — from a regional planning scenario and from a deterministic model. Results indicate the mean daily streamflow in the Jordan River watershed will increase by an amount ranging from 11.2% to 14.5% in the 2040s and from 6.8% to 15.3% in the 2090s. The respective increases in sediment load in the 2040s and 2090s is projected to be 6.7% and 39.7% in the canyons and about 7.4% to 14.2% in the Jordan valley. The historical 50th percentile timing of streamflow and sediment load is projected to be shifted earlier by three to four weeks by mid-century and four to eight weeks by late-century. The projected streamflow and sediment load results establish a nonlinear relationship with each other and are highly sensitive to projected climate change. The predicted changes in streamflow and sediment yield will have implications for water supply, flood control and stormwater management.

(KEYWORDS: hydrologic modeling; climate downscaling; land use modeling; snowmelt; sediment; uncertainty.)

INTRODUCTION

It is known that streamflow and water quality parameters from a watershed change dynamically over time and space. Results from climate model simulations suggest that higher mean temperatures will decrease snowpack storage and lead to earlier melting of snowpack in the higher-elevation mountain ranges of Western North America (Mote et al. 2005). Other regional studies have also indicated decreases in snow accumulation and earlier melt in the Sierra Nevada Mountains and through the western United States (U.S.) (Kapnick and Hall 2012; Burke and Ficklin 2017; Mote et al. 2018). Moreover, the impact of climate change on mountain hydrology has already been observed in the western U.S., with changes in streamflow resulting from earlier snowmelt and more precipitation falling as rain (Stewart et al. 2005). The amount of snowpack depends on both the temperature and the amount of precipitation. At higher elevations snowpack is primarily sensitive to the amount of precipitation, while at lower altitudes it is mainly sensitive to the temperature. As indicated by Scalzitti et al. (2016a), the elevation threshold between these two regimes is expected to lower by up to 300 m by

Paper No. JAWRA-18-0143-P of the *Journal of the American Water Resources Association* (JAWRA). Received October 13, 2018; accepted August 27, 2019.

Department of Civil & Environmental Engineering (Khatri), Department of Atmospheric Sciences (Strong, Kochanski), and Department of City & Metropolitan Planning (Buchert), University of Utah, Salt Lake City, Utah, USA; and Division of Water Quality (von Stackelberg), Utah Department of Environmental Quality, Salt Lake City, Utah, USA (Correspondence to Khatri: krishna.khatri@gmail.com).

Citation: Khatri, K.B., C. Strong, N. von Stackelberg, M. Buchert, and A.K. Kochanski. 2019. "Impact of Climate and Land Use Change on Streamflow and Sediment Yield in a Snow-Dominated Semiarid Mountainous Watershed." *Journal of the American Water Resources Association* 1–24. https://doi.org/10.1111/1752-1688.12803.

the end of this century leading to reduced water accumulation and increased runoff. As the flow regime changes, the process of erosion and sedimentation in watersheds (strongly related to rainfall and runoff processes) will change as well, leading to changes in the timing and concentration of sediment (Francipane et al. 2015).

Erosion and sedimentation, in a watershed, are closely related to natural processes, driven mainly by rainfall and runoff processes. Erosion is the detachment and movement of soil particles by natural forces, primarily water and wind. Sediment yield is the amount of soil detached and transported to surface water bodies within a time scale over a specific area (Issaka and Ashraf 2017). Sediment yield in a watershed varies spatially, depending on several contributing factors including topography, type of soil, catchment area, climate (i.e., precipitation, wind, temperature etc.), vegetation cover, human-influenced soil erosion, forest fires, river discharge (Francipane et al. 2015). In a watershed, the amount of sediment transported by a river system depends on the supply of sediment and transport capacity of the flow. Therefore, the accuracy of the estimate of the sediment yield from any watershed relies on understanding and representation of the multiple contributing factors such as rainfall, runoff, and erosion processes. More discussion on sedimentation processes can be found in earlier publications (e.g., Pimentel et al. 1997; Kalin and Hantush 2006; Wilkinson and McElroy 2007; Francipane et al. 2015).

Streamflow and water quality parameters, including nutrients, sediment, and temperature of watersheds, vary over time and space. The variability of flux is driven by social, environmental, and economic factors (Russell et al. 2008). Climate and land use and land cover (LULC) change are considered to be the main two drivers affecting water quantity and quality in watersheds and waterways (Ahearn et al. 2005; Ficklin et al. 2014; Kaushal et al. 2014; Kharel et al. 2016). Climate change modifies local hydrological processes, which have direct and indirect impacts on water quality and streamflow. LULC change affects hydrological processes including interception, infiltration, evapotranspiration, and resulting alterations of surface and subsurface flows. Investigation of land use and water quality relationships is particularly useful in the case of pollution from diffused urban and agricultural sources (Allan et al. 1997; Baker 2005). Streamflow and sediment yields are expected to change with climate perturbations and other social changes (e.g., urbanization), however, these changes can be nonlinear and watershed-specific and can be difficult to generalize for other areas (Nunes et al. 2013).

Earlier studies have developed either regression-based models (Tong and Chen 2002; Williams et al. 2014; Tasdighi et al. 2017) or hydrological models (Ficklin et al. 2014; El-Khoury et al. 2015; Dudula and Randhir 2016) to study these relationships and analyze the impacts. The majority of these studies concluded that strong correlations exist between water fluxes and land use types and climate change; however, significant differences can be expected between wet and dry years (Tasdighi et al. 2017).

The sediment yield per unit area and sediment delivery ratio decrease as the basin characteristics change (Parsons et al. 2006). As basin size increases, the slope and channel gradients decrease, resulting in changes in the energy available for sediment transport (Birkinshaw and Bathurst 2006). Therefore, interactions between changing climate and varying land use, vegetation, and geology in complex mountainous watersheds are expected to have a direct impact on the streamflow generation and sediment load. Most earlier sediment load assessments typically used daily precipitation totals (Coulthard et al. 2012; Routschek et al. 2014) despite the fact that a higher-resolution characterization of rainfall is warranted for climate impact assessment studies (Mullan 2013). A recent study on consequences of climate change for the reliability of Salt Lake City's water supply systems recommended future research work to undertake sensitivity and scenarios analysis using updated climate projections and dynamically downscaled, high-resolution climate model simulations to improve representation of hydroclimatic interactions associated with specific topographic features of the local watersheds (Bardsley et al. 2013).

The overall objective of this study was to investigate the impact of climate and LULC change on streamflow and sediment yield in snow-fed mountainous watershed in a semi-arid region with uncertainty. The specific objectives were (1) to analyze the sensitivity of the magnitude and timing of streamflow and sediment yield due to changing climate and LULC in the near-future (a decadal analysis for years 2035–2044, hereafter 2040s) and the far-future (a decadal analysis for years 2085–2094, hereafter 2090s), and (2) to establish relationships between streamflow and sediment concentration from short-reach and snow-fed watersheds in years 2040s and 2090s. The case study considered in this work is the Jordan River valley watershed in Salt Lake County, Utah, which has mountainous headwaters with snowmelt-dominated streamflow, coupled with a fast-growing urbanized area in the valley.

The results reported in this paper, include two locations of the Jordan River watershed: (1) Big Cottonwood Creek at the Canyon Mouth for climate change impact and (2) above the Surplus Canal in

the Jordan River for climate and LULC change impact. The Big Cottonwood Creek subwatershed is the upper parts of the Jordan River, primarily covered by scrub shrub and forests. There is no settlement upstream of the Big Cottonwood Creek streamgage site, so future streamflow and sediment yield will be impacted by only climate change. It is expected that the future growth of the urban areas will be toward the southern and western areas of the county. Therefore, the Jordan River site was evaluated for impact of climate and LULC changes. A scenario approach was applied to perform three decades of hourly simulations of three scenarios of climate and LULC changes using a physically based hydrologic model (HSPF [Hydrological Simulation Program — FORTRAN]). The daily results were obtained by aggregating the hourly simulated results of the HSPF model. The results presented are based on the average of ten simulated years of 2000s (Jan 1995–Dec 2004), 2040s (Jan 2035–Dec 2044) and 2090s (Jan 2085–Dec 2094).

HSPF MODEL

The HSPF model is a physically based hydrological and continuous simulation model (Bicknell et al. 2001) developed by the U.S. Environmental Protection Agency (USEPA). HSPF simulates water quantity and quality at user-specified spatial and temporal scales. The model can simulate time steps from subhourly through daily to monthly, with a duration of a couple minutes to hundreds of years (Bicknell et al. 2001). The model can assess the effects of urbanization, reservoir operations, point and nonpoint source pollutant loadings, and flow diversions. The HSPF model has been used for flood control planning and operations, river basin and watershed planning, storm drainage analysis, point and nonpoint source pollution analyses, soil erosion and sediment transport studies, evaluation of urban and agricultural best management practices and study of pesticides, nutrients, and toxic substances (Duda et al. 2012; Dudula and Randhir 2016).

The HSPF framework is developed modularly with three major components: (1) PERLND — for watershed processes on pervious land areas, (2) IMPLND — for processes on impervious land areas, and (3) RCHRES — for processes in streams and vertically mixed lakes. It models hydrology as a water balance in multiple surface and subsurface layers and is typically implemented in large watersheds at an hourly time step. The water balance (Equation 1) is simulated based on Philip's infiltration (Bicknell et al. 2001) coupled with multiple surface and subsurface stores (e.g., interception storage, surface storage, upper zone soil storage, lower zone soil storage, active groundwater, inactive [deep] groundwater).

$$R = P - \mathrm{ET} - \mathrm{IG} - \Delta S, \tag{1}$$

where P is the precipitation, R is the runoff, ET is the evapotranspiration, IG is deep/inactive groundwater, and ΔS is change in soil storage. The snowmelt process used in this study was the temperature index/degree approach (Equation 2).

$$Q = K_{\mathrm{melt}}(T_{\mathrm{air}} - T_{\mathrm{base}})S_{\mathrm{cov}}, \tag{2}$$

where Q is equivalent melt, K_{melt} is the degree day factor, T_{base} is the reference temperature for snowmelt, and S_{cov} is fraction of land segment covered by snow.

Sediment behavior within a watershed system includes loading and erosion sources, delivery of the eroded sediment sources to streams, drains, and other pathways. Sediment erosion in HSPF uses a method that is similar to the Universal Soil Loss Equation (USLE) sediment-detachment approach coupled with transport capacity based on overland flow. The USLE, developed in the 1970s by the U.S. Department of Agriculture, is an empirical soil erosion model used widely to provide annual estimates of soil erosion from hillslopes. The model has undergone much research and a number of modifications such as Revised-USLE and modified version of the USLE. More discussion on the original USLE conception and equation, updates, and application examples are available in earlier publication (e.g., Renard et al. 2011; Benavidez et al. 2018).

HSPF simulates three sediment types (sand, silt, and clay) in addition to organic chemical and transformation products of that chemical. The sediment loading and routing in HSPF, similar to other watershed models, does not account for the stream bed load. The three options of sand transport in waterbodies included in the HSPF model are the Toffaleti method, Colby method, and Power functions. Here, we apply the Power function:

$$P_{\mathrm{s}} = K_{\mathrm{s}} V_{\mathrm{a}}^{b}, \tag{3}$$

where P_{s} is potential sand concentration, V_{a} is average stream velocity, K_{s} is the intercept or coefficient to input parameter, b is the exponent input parameter. Scour and disposition for cohesive sediments (i.e., silt and clay) in waterbodies is handled using a critical shear stress value:

$$\tau_c = \theta(\gamma_s - \gamma)D, \quad (4)$$

where θ is the dimensionless Shields parameters for entrainment of a sediment particle of size D, γ_s is the unit weight of bed sediment, and γ is the unit weight of water. Readers can find a detailed description of the model structure, all governing equations, data requirements, application examples, technical notes, and the model calibrations processes elsewhere (Bicknell et al. 2001; Al-Abed and Whiteley 2002; Donigian 2002; Duda et al. 2012; Dudula and Randhir 2016).

MATERIALS AND METHODS

This study adopts the multiple scenario approach to analyze the impact of future climate and LULC changes on streamflow and sediment yield, which is a commonly used method for analyzing long-term uncertainties that are not readily quantifiable (Arnell and Lloyd-Hughes 2014; Moss et al. 2010; Khatri 2013; Khatri et al. 2018). More discussion on the scenarios approach and application in futurist studies are available in earlier studies (e.g., Arnell and Lloyd-Hughes 2014; Hejazi et al., 2014; Simonovic 2017). The HSPF model was used to simulate streamflows and sediment concentration based on forcing by future climate change projections and LULC changes in the watershed.

Three climate scenarios were generated using statistically downscaled and dynamically downscaled climate data (see climate section). Future LULC changes were projected using three land use change scenarios (see land use section). Earlier studies have adopted snowmelt-dominated streamflow timing by assessing trends in the date of the center of mass for flow (McCabe and Clark 2005; Stewart et al. 2005; Hodgkins and Dudley 2006), the start day of the snowmelt runoff (Stewart et al. 2005), or the day at which each percentile of the annual flow occurs (Moore et al. 2007). This study adopts the date of the center of mass for flow (i.e., a 50th percentile of cumulative annual streamflow) to assess the timing of the snowmelt-dominated streamflow and sediment load.

We performed sensitivity analysis to determine the relative impact of climate and LULC change on streamflow and sediment concentration. This was undertaken by evaluating the change in streamflow and sediment load with respect to (1) change in LULC only (without changing climate parameters), (2) change in climate only (without changing LULC parameters), and (3) combined change in climate and LULC. Each of the LULC scenarios was also simulated separately with each climate change scenario to identify the most impactful LULC change scenario. The sensitivity analysis was undertaken at the Jordan River site which has the potential impact of LULC change. The relationships between streamflow and sediment concentration at both the sites were established by regressing the projected future streamflows and corresponding sedimentation concentration for the years 2040s and 2090s. Further discussion of the objectives and methods of sensitivity analysis in general are available in Arnold et al. (2012) and Zeckoski et al. (2015) and references therein.

Study Area

The Jordan River valley watershed encompasses most of Salt Lake County, Utah (Figure 1). It remains the most populous county in Utah with 1.1 million residents — which is one third of the total population of the state (Utah Governor's Office of Management and Budget 2012). The watershed is bounded by the Wasatch Mountains on the east, the Oquirrh Mountains on the west, the Traverse Range on the south, and the Great Salt Lake on the northwest. About 958 square kilometers (46% of the land) in the watershed are in rugged mountain ranges and are largely undevelopable. Approximately 348 km^2 (17%) of the Wasatch Mountains are protected to ensure drinking water quality for Salt Lake City and Sandy City. The valley portion is largely an urbanized area, whereas the higher elevations are less developed but considerably impacted by mining and recreational activities.

The Jordan River originates as the outflow from Utah Lake to the south, flows north into and through the county (about 80.50 km) and discharges into the hypersaline Great Salt Lake. The Jordan River is fed by several canyon streams flowing from the Wasatch and Oquirrh Mountain ranges into the river as it makes its way north. The hydrology of the Jordan River is highly regulated and unnatural, impacted by Utah Lake releases, wastewater effluent, stormwater, irrigation return flow, groundwater, and snowmelt from the mountains (Salt Lake County 2017). Water supply diversions from the canyons at the valley support about two thirds of the drinking water demand of the Jordan valley (Bardsley et al. 2013). The Jordan River supports and maintains the ecosystems of the valley and also contributes more than 20% of the Great Salt Lake freshwater inflow (Wurtsbaugh et al. 2016).

As stated earlier, the analysis and results presented in this paper include two sites: Big Cottonwood Creek subwatershed at the Canyon Mouth and

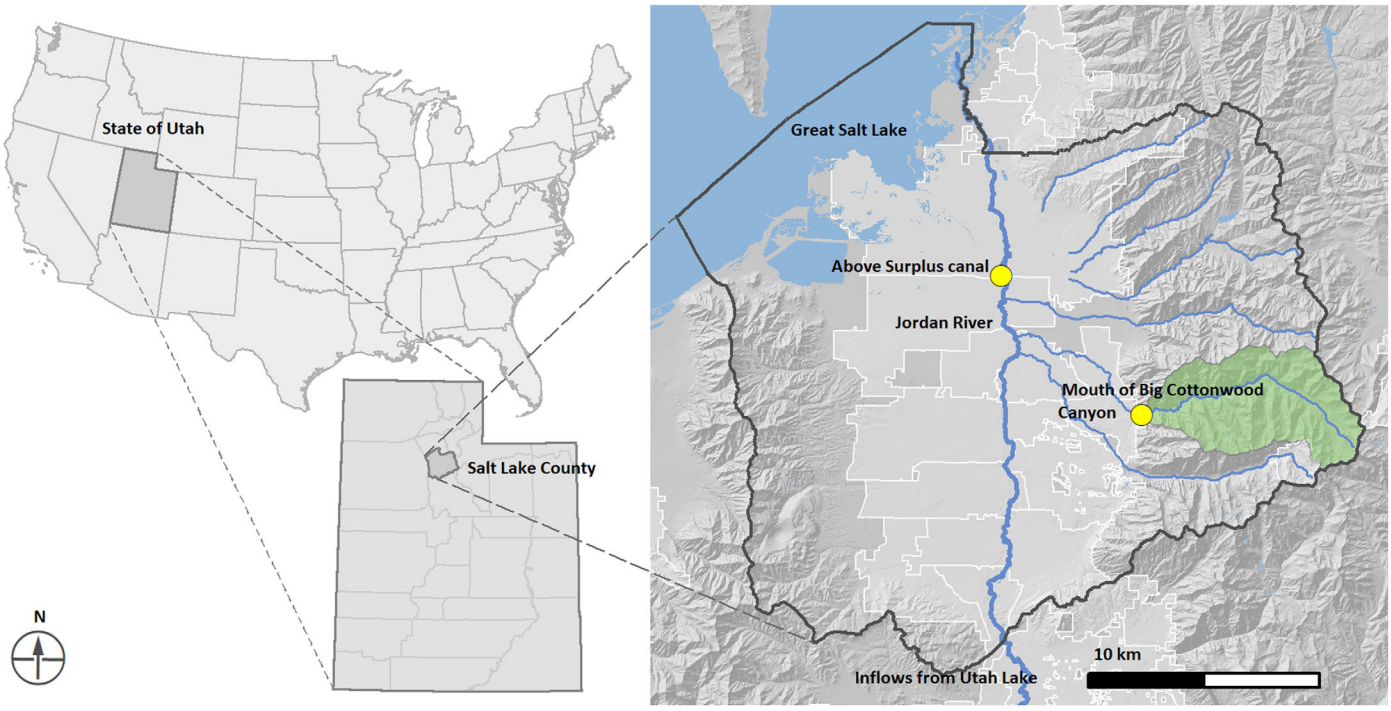

FIGURE 1. Study area: Jordan River watershed in Salt Lake County, Utah. The two filled circles represent the streamgage locations of Big Cottonwood Canyon and Jordan River above the surplus canal.

the Jordan River above the surplus canal (see location dots in Figure 1). The upper parts of the canyons are mountainous having elevations ranging from 1,960 to 2,607 m. The forest area of Big Cottonwood (upper mountain area) is about 129.24 km^2 and has an average slope of 50.8%. There is limited development upstream of the Big Cottonwood canyon mouth and the streamflow is influenced primarily by the snow hydrology. Therefore, the upper Big Cottonwood subwatershed was selected to evaluate the impacts of climate change. The other location considered for the analysis is just above the Surplus Canal in the Jordan River, which has a potential to be influenced by climate and LULC change (see Figure 1).

HSPF Model Development

This study updated the HSPF model built by Stantec Consulting Inc. under a contract to Salt Lake County Watershed Planning and Restoration, supported by a grant from the Utah Department of Environmental Quality. The model was developed using the HSPF program (Version 12) under the Better Assessment Science Integrating Point and Nonpoint Sources (BASINS; Version 4.1 modeling platform). The entire watershed was delineated into 17 major watersheds, 27 subwatersheds, and 197 separate subbasins (i.e., which are equivalent to the smallest hydrologic response unit) to match the 2009 Water Quality Stewardship Plan of the County (Figure 2). The factors considered in the basin delineation include topographic relief, stormwater infrastructure, irrigation canal drainage, major points of diversion for the water supply systems, flow exchange locations where canals cross tributaries, streamflow gages, and water quality sampling stations (Stantec Consulting Inc 2011).

The model has eight meteorological segments and three segments with hydrologic soil groups: B indicates soils with a moderate infiltration rate when thoroughly wet, C indicates soils with a slow infiltration rate when thoroughly wet, and D indicates soils with a very slow infiltration rate and high runoff potential when thoroughly wet. These soil groups are specified based on Soil Survey Geographic Database data provided by the Natural Resources Conservation Service. Topographically, the model has ten segments that divide the elevation ranging from a low elevation (~1,350 m) to a high elevation (~2,290 m). More discussion on the model development processes including model delineation and segmentation is available in the original model report (Stantec Consulting Inc 2011).

Model Inputs, Evaluation Data, and Sources

The model report discusses all the input data used for the base model development and their sources

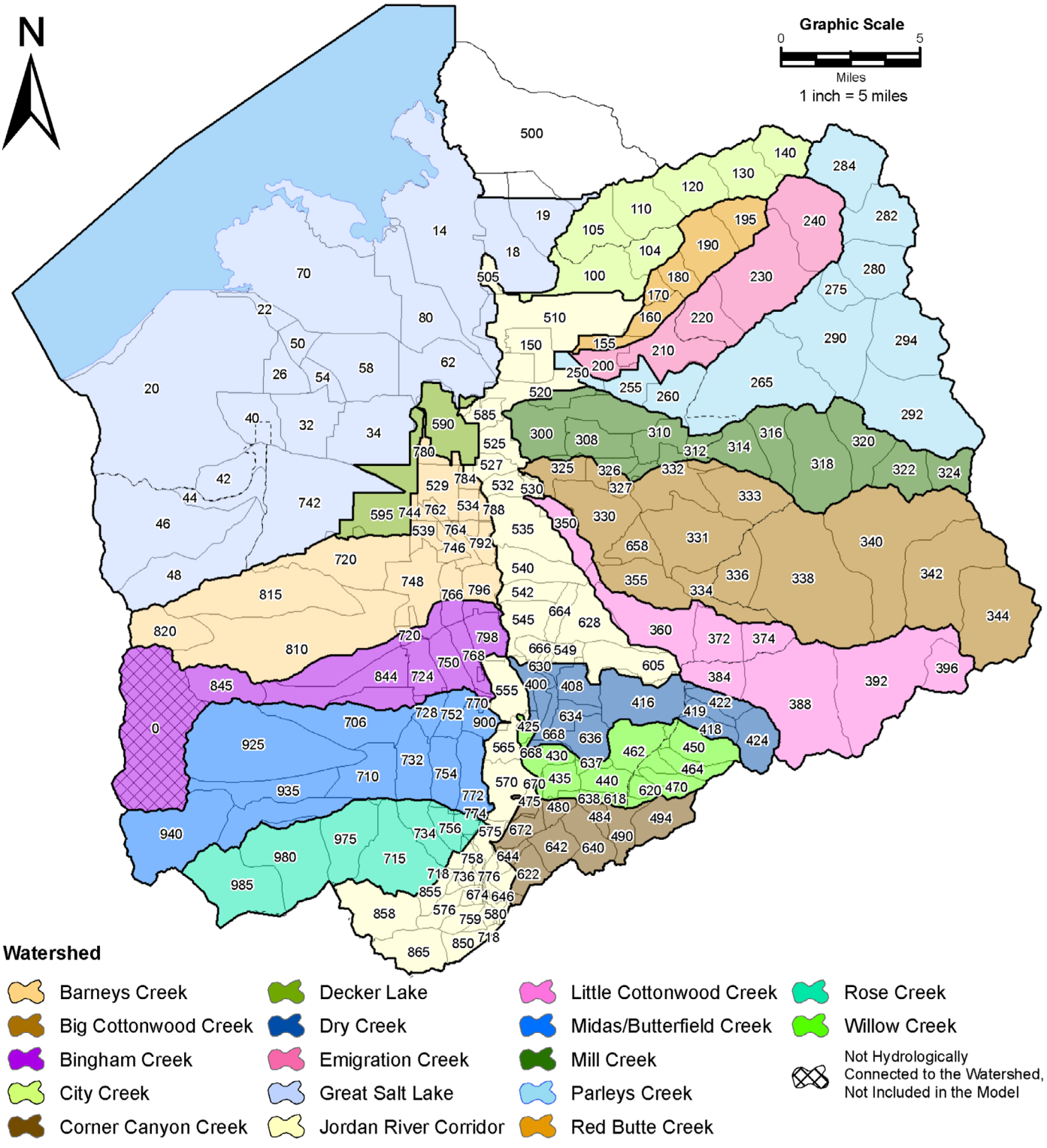

FIGURE 2. Delineation of the Hydrological Simulation Program — FORTRAN (HSPF) model for the Jordan valley watershed.

(Stantec Consulting Inc 2011). Table 1 summarizes the main model input data including future conditions, model performance evaluation data, and data sources.

HSPF Model Calibration and Validation Approach

The "weight of evidence" approach was applied to evaluate the performance of the model, which utilizes

TABLE 1. A summary of input data used for developing the HSPF model, calibration, validation, and future scenarios.

Description of data	Sources
Meteorological data, digital elevation model, soil data, river network, and water quality data.	Downloaded from the USEPA database, which contains more than 1,600 stations in the U.S., using the BASINS tool. https://www.epa.gov/sites/production/files/2015-07/documents/exercise-1-basins-download-tool-and-data-extensions.pdf
Land use and land cover (LULC) data	BASINS manage the land use database from National Land Cover Dataset (NLCD). The downloaded land use map (The 2001 NLCD for Salt Lake County) was also adjusted based on the updated map available in Salt Lake County that was developed for the Engineering and Flood Control Division's stormwater monitoring program in 2000. An inventory of agricultural lands, the types of crops, and whether they are irrigated or not irrigated was developed by the Utah Division of Water Resources. https://gis.utah.gov/data/planning/water-related-land/
Reservoir, detention basin, water diversion, irrigation drainage, and return flows	Salt Lake City Public Utilities, South Valley Water Reclamation Plant, Central Valley Water Reclamation Plant, South Davis South Water Reclamation Plant, Salt Lake City. Water Reclamation Plant, and Magna Water Reclamation Plant. Irrigation canal diversion records obtained from Utah Division of Water Rights.
Snowpack	Historical Snowpack data download from BASINS tool that are based on the SNOTEL observations of Natural Resources Conservation Service (NRCS).
Potential evapotranspiration	PET used in this model was obtained from the BASINS system and updated with the results of Strong et al. (2017).
Groundwater	Groundwater base flows obtained from MODFLOW model developed by U.S. Geological Survey (USGS; see model report).
Streamflow	Streamflow data used for the model calibration and validation were downloaded from (1) Salt Lake City Public Utility gage for Big Cottonwood Creek, (2) USGS gage 10170490 for Jordan River and Surplus Canal.
Sediment data	The sediment data used for the calibration were collected by Utah Division of Water Quality.
Future land use	Future LULC data were obtained from the LULC modeling from this study (see LULC section).
Future climate data	Dynamically and statistically downscaled (see climate section).

Notes: U.S., United States; USEPA, U.S. Environmental Protection Agency; BASINS, Better Assessment Science Integrating Point and Nonpoint Sources; SNOTEL, SNOpack Telemetry; MODFLOW, Modular Three-Dimensional Finite-Difference Groundwater Flow Model.

multiple graphical comparisons and statistical tests to evaluate model performance (Donigian 2002; Donigian and Love 2003). In this approach, several hydrologic characteristics were evaluated, including annual water balance, snow depth, and annual and monthly flow volumes, and graphical comparisons were made of flow hydrographs, flow duration curves, and mean daily flow via scatter plots with linear regression (Stantec Consulting Inc 2011). Several technical notes available at the USEPA website (e.g., https://www.epa.gov/ceam/basins-technical-notes) such as "BASINS Technical Note 8: Sediment parameter and calibration guidance for HSPF" were considered to calibrate and validate the HSPF model.

The model calibration period includes years with dry, normal, and wet precipitation levels. The model was calibrated for years Jan 1, 1995 through Dec 31, 2004 and validated for years Jan 1, 2005 through Dec 31, 2006 (only for the hydrological simulations and not for the sediment concentration due to lack of observed data).

The base model was calibrated for 17 sites including three sites for the snow calibration, seven sites for flow calibration, and seven sites for water quality (see Stantec Consulting Inc 2011). This updated model calibration was further extended for more sites (e.g., six creeks) and the performances were evaluated using percent bias (PBIAS) measure and Nash–Sutcliffe efficiency (NSE) coefficient in addition to the coefficient of determination (R^2) used in the base model. The two calibration sites reported in this paper (i.e., Big Cottonwood and Jordan River above surplus canal) were calibrated at the time of the base model development.

HSPF Model Performance Metrics

The three statistical parameters considered for the model evaluation are the R^2, PBIAS measure and NSE coefficient, all of which are commonly used statistical parameters for hydrological model calibration. The R^2 ranges from 0 to 1, with higher values indicating less error variance, and typically values >0.5 are considered acceptable. The optimal value of PBIAS is 0.0%. Positive values of PBIAS indicate model underestimating bias, and negative values indicate model overestimating bias (Gupta et al. 1999). The NSE value ranges from $-\infty$ to 1.0, with 1.0 being the optimal value. Values ≤ 0 are considered poor value indicating the simulated results depart substantially from mean observed values (Moriasi et al. 2007). The targeted statistics of model evaluations depend on the type and intended use of the model (Harmel et al. 2014; Daggupati et al. 2015). More detailed guidance on model evaluation

techniques, selection of specific statistics, ranges of model calibration parameters, and recommended ranges of model performances for hydrology and water quality parameters including sediment load are available in several publications (e.g., ASCE 1993; Donigian 2002; Borah and Bera 2004; Moriasi et al. 2007; Duda et al. 2012; Daggupati et al. 2015).

Future Climate and LULC Change Scenarios

Future Climate Modeling. Climate inputs for the HSPF model included hourly precipitation, air temperature, dew point temperature, wind speed, cloud cover, radiation, and potential evaporation. The historical climate data for years Jan 1, 1995 to Dec 31, 2006 were downloaded through EPA BASINS (USEPA 2007). Future climate inputs were derived from dynamically downscaled and statistically downscaled global climate model output as detailed in two sections below. The statistical downscaling (Reclamation 2013) was based on more than 20 global climate models forced by four greenhouse gas emission scenarios, referred to as Representative Concentration Pathways (RCPs; Vuuren et al. 2011). For the dynamical downscaling, the high computational expense of our regional climate model configuration (Scalzitti et al. 2016a, b) limited the simulation to a mid-century decade (2035–2044) and a late-century decade (2085–2094), both under the moderate greenhouse gas emission scenario RCP6.0. For consistency, we focus on climate inputs for the same two decades in the statistical downscaling archive.

Using future periods of 10 years is shorter than the conventional 20–30 years used for a climatology, where the latter is specified to narrow confidence limits on estimated statistics and to encompass natural variations which may be multi-decadal in their periodicity. Nonetheless, the statistical downscaling ensemble used here has more than 20 global climate models which were forced by atmospheric composition, but otherwise freely evolved forward over several decades from their initial conditions, thus achieving a broad range of natural variability states (e.g., Deser et al. 2012). In this way, our representation of the mid-century and late-century climate state achieved a large sample size and encompassed natural variations by using many models rather than many decades.

Dynamic Downscaling Using the WRF Regional Climate Model. Hourly meteorological inputs for HSPF were dynamically downscaled to 4-km horizontal resolution using the Weather Research and Forecasting (WRF) model (Skamarock et al. 2005). Full details on the WRF model configuration and historical validation are presented in (Strong et al. 2014; Scalzitti et al. 2016b), and analysis of the future simulation is presented in Scalzitti et al. (2016a). The simulations were run using three nested domains with horizontal resolutions increasing from 36-km for the outermost domain, through 12-km intermediate domain, to 4-km innermost domain encompassing Utah. As noted in the preceding section, historical years 1989–2010 as well as two future decades (2035–2044 and 2085–2094) were simulated under the RCP6.0. Boundary conditions for the dynamical downscaling were derived from the National Center for Atmospheric Research (NCAR) Community Climate System Model, selected based on its skill in capturing observed relationships between study-region precipitation and modes of variability such as El Niño (Smith et al. 2015). The dynamically downscaled results were spatiotemporally interpolated to eight stations selected in the Jordan River valley watershed.

Dynamically downscaled data contain biases, so a change factor approach was used, meaning that climate change perturbation signals generated by WRF were used to offset historical temperatures and to scale historical precipitation (e.g., Zahmatkesh et al. 2014). Mitigating model bias is especially important because the HSPF framework was calibrated to observations. A disadvantage of the change factor method is that it assumes future persistence in historical storm occurrence frequencies and trajectories. The benefit of this method though, comes from the fact that it enables direct comparison of a future year to the corresponding historical year perturbed by the climate change factors. We use ΔT_{2040} to denote the temperature offset used for the mid-century decade (2035–2044) relative to the historical reference period (1985–2004). ΔT_{2040} derived from WRF is specific to each hour of year and each weather station location used to calibrate HSPF. ΔT_{2040} was smoothed by fitting the first two harmonics of the annual cycle. The perturbed future temperatures for 2035–2044 were then generated by adding ΔT_{2040} to hourly temperatures during each year of the historical period from 1995 to 2004. We used the same method to produce future temperatures for 2085–2094, and the smoothed offsets for this late-century decade are denoted by ΔT_{2090}.

Precipitation was treated analogously except that ratios were used rather than differences. We use fP_{2040} to denote the ratio given by mid-century (2035–2044) monthly precipitation divided by historical monthly precipitation (1985–2004). Perturbed future precipitation amounts were generated by multiplying fP_{2040} by the hourly precipitation during each year of the historical period from 1995 to 2004. The same calculations were applied for the 2090 period using the factors fP_{2090}.

Statistical Downscaling. To provide context for the dynamical downscaling results from WRF, we forced HSPF with the broader range of climate change outcomes captured by CMIP5 (The Coupled Model Intercomparison Project Phase 5; Taylor et al. 2012). CMIP5 results were statistically downscaled via Bias Correction Spatial Disaggregation (BCSD) method (Reclamation 2013) for all four RCPs (2.6, 4.5, 6.0, and 8.5), totaling 231 simulations from more than twenty global climate models. To quantify how the warmest and wettest, and also coolest and driest, conditions in this ensemble of 231 simulations would affect sedimentation in the study region, we analyzed upper and lower quartiles of the 231-member ensemble. Quartiles of the entire ensemble were used because the precipitation change variability in the study region is organized more by inter-model contrasts than by RCP. These inter-model differences stem in part from contrasts in storm track strength (Chang et al. 2012) and the study region is very close to the zero isopleth of ensemble mean future precipitation change when analyzing individual RCPs (e.g., Smith et al. 2015). Because the BCSD data are coarser in resolution (14-km horizontal) than WRF, there are only three grid points in the headwaters and we used average changes across the Jordan River basin rather than interpolating to individual weather station locations. Resulting temperature offsets (ΔT_{2040} and ΔT_{2090}) and precipitation scaling factors (fP_{2040} and fP_{2090}) are presented below in the results section.

Future LULC Modeling

Three sets of future LULC changes scenarios considered are: (1) the continuation of the existing LULC, (2) business-as-usual-growth (BUG) LULC change, and (3) centers-oriented-growth (COG) LULC change. The continuation of the existing LULC scenario will be supported by the existing LULC modeled on the base model (see report, Stantec Consulting Inc 2011). For the other two scenarios, the baseline is based on a land use classification produced by Salt Lake County. This classification used the National Land Cover Dataset to assign land cover in the East and West mountainous areas surrounding the Jordan Valley. For the developed valley bottom, water land use was assigned based on the State Division of Water Resources' Water-related Land Use database. Both scenarios have connections to the region's nationally recognized culture and practice of bottom-up, collaborative regional planning (Burbidge et al. 2007). The two scenarios were applied to the urbanized valley; no change was considered to the LULC in the mountains.

BUG Scenario-Based Spatial Interaction Model. The BUG land use scenario was developed for use by the Wasatch Front Regional Council (WFRC), Salt Lake County's designated Metropolitan Planning Organization, which is in the multi-year process of building and calibrating a state-of-the-art urban growth model using the UrbanSim platform (Waddell 2011). During this period, WFRC has had no objective trend growth land use scenarios for benchmarking regional alternative scenarios (the scenario-building process used by WFRC, while state-of-the-practice for regional land-use planning, is not a robust predictor of trend growth). As an interim solution, researchers at the University of Utah's Metropolitan Research Center developed a spatial attraction model of Greenfield and infill development. Following methods of Ewing and Bartholomew (Ewing and Bartholomew 2009), logistic regression models for each of five land-uses (retail, other employment, industrial, single family residential, and multi-family residential) were estimated for the log odds of a parcel having a given land use in 2015. Predictor variables included surrounding land uses and parcel accessibility to regional population and employment. The resulting empirical models were applied to all 2015 vacant parcels, but with accessibility measures now derived from WFRC's travel demand model reflecting 2040 road and transit networks. Population and employment were then allocated sequentially on a parcel-by-parcel basis, in decreasing likelihood of development (across all four development land use classes) and using official county-scale projections (Utah Governor's Office of Management and Budget 2012) as control totals.

COG Scenario-Based Normative Growth Model. The COG scenario was developed for the metro regions' currently adopted transportation plan (Wasatch Front Regional Council 2015), where it is the land-use basis for the transportation modeling used to plan transportation spending and air quality conformity over the 2015–2040 time period. It was developed by WFRC via a process of coordination and participative planning with municipal and county governments that reflects both official State-produced population and employment growth projections, and municipal/county General Plans. The COG plan focuses one-third of the county's projected growth into development centers occupying just 3% of the growth areal footprint, thus reducing the total acreage of impacted land (Wasatch Front Regional Council 2010). Scenario development utilized Envision Tomorrow — a planning support system that takes interactive GIS (geographic information systems) accounting framework that in addition to population and employment, estimates physical building size and lot

coverage, including total lot impervious fraction, for each parcel with changed land-use in the scenario (Fregonese Associates 2015).

We used Envision Tomorrow outputs of impervious fraction and redevelopment intensity, in conjunction with baseline impervious fraction from the HSPF model, to estimate impervious area added through development. As well as development of urban and rural undeveloped lands, the COG scenario and the Envision Tomorrow tool also explicitly model redevelopment of previously developed land; where this occurred, we accounted for gross impervious area gains and losses.

RESULTS

Model Calibration and Validation

The three statistical parameters considered for the model evaluation are the R^2, PBIAS measure and NSE coefficient. Figure 3a and 3c compare simulated daily streamflow with observed data at the Big Cottonwood Canyon site and Jordan River site with calibration results. The validation statistics for the hydrology (figures not included) were also found to be similar to the calibration (e.g., Big cottonwood: $R^2 = 0.78$, NSE = 0.64 and PBIAS = −12.6%, and Jordan River: $R^2 = 0.87$, NSE = 0.86, and PBIAS = 0.75%). Figure 3b and 3d presents the calibration results for the sediment yield at the Big Cottonweed and Jordan River stations.

The hydrologic performance of the model at both of the sites is in the good range. However, the model performance on the sediment concentration at both stations are in the poor range. Unlike streamflow data, the available sediment data for most of the sites were sporadically collected grab samples and were not continuously observed (see Figure 3). Discontinuously observed data may not capture all the sediment flow as a few major storms during the year can result in significant sediment load (Donigian 2002). With the caveat of potentially poor performance due principally to limited observations, the sediment calibration results were accepted for watershed planning. Other publications (e.g., Moore et al. 1988; Engelmann et al. 2002; Borah and Bera 2004; Diaz-Ramirez et al. 2011) on sediment modeling using HSPF and other hydrologic models have discussed challenges due to the lack of observed data, complexity of the sediment loading, and sediment transport, and outline various reasons for poor model performances (i.e., the lower R^2 and negative NSE; see conclusion of Engelmann et al. 2002). Moreover, the intended use of this model was to support the watershed planning by simulating multiple distinct future scenarios. The three categories of intended model use commonly reported in the published literature are: exploratory, planning, and regulatory/legal. As recommended in earlier publications (e.g., Harmel et al. 2014; Daggupati et al. 2015), the planning category includes modeling for planning purposes in which confidence in the model's ability to capture scenario differences is important, but very high accuracy and precision in model predictions are less critical.

Changes in Land-Use and Land-Cover Type

Modeled 2010–2040 LULC changes show differences in overall magnitude as well as spatial distribution between the BUG and COG scenarios. The BUG scenario results in more diffused development throughout the model domain, with highly impervious commercial and industrial uses occurring exclusively on previously undeveloped land. This is an artifact of the BUG land-use change model's selective spatial footprint, of previously undeveloped land. In contrast, the COG model — conceptually intended to focus new development onto a limited spatial footprint and cluster growth into centers — locates highly impervious business land use preferentially in previously developed areas, where new impervious surface produces a smaller net change. This scenario also disproportionately allocates low-density residential development to the large remaining open tracts of land on the south-west margin of the valley, where the low impervious fraction of this land use type also makes for a relatively small change to the baseline stocks of impervious land area. We estimate that from a 2010 baseline of 342 km^2 impervious surface (out of a total land area of 1,948 km^2), urban growth in the BUG scenario would result in the conversion of a net 65 km^2 from pervious to impervious surface, compared with a net conversion of 10 km^2 in the COG scenario (Figure 4).

Climate Perturbations

Smoothed mid-century temperature perturbations ($\underset{2040}{\tilde{\Delta T}}$) for the eight stations averaged 2.7°C with the strongest warming in the late winter and late summer months (Figure 5a). For the late-century decade, $\underset{2090}{\tilde{\Delta T}}$ averaged 5.4°C with a similar annual cycle to the anomalies (Figure 5b). The mid-century precipitation scaling factors ($\underset{2040}{\tilde{fP}}$) averaged 1.3 with larger values

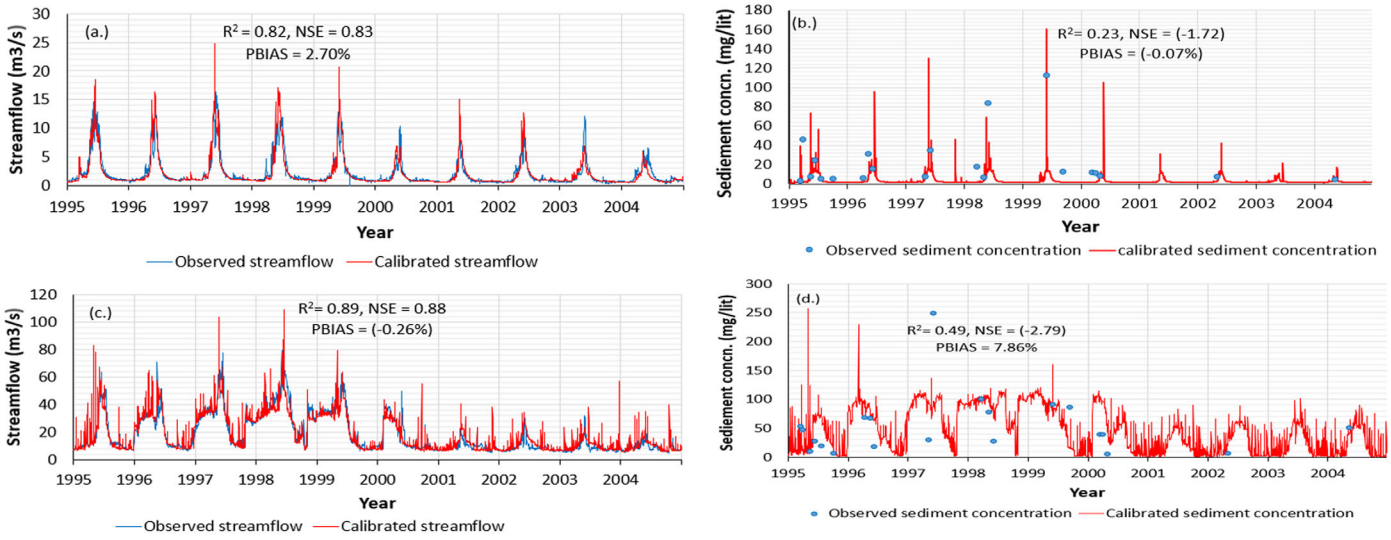

FIGURE 3. Observed and simulated daily streamflow and sediment load at the Big Cottonwood Canyon mouth (a,b) and above Surplus Canal in the Jordan River (c,d). R^2, coefficient of determination; PBIAS, percent bias; NSE, Nash–Sutcliffe efficiency.

in the winter and late summer months (Figure 5c). The precipitation scaling factors averaged 1.2 for the late-century decade ($\tilde{fP}_{2090}$) (Figure 5d). The large relative increase in precipitation during the summer months is small on an absolute basis because the summer months are relatively dry. That $\tilde{fP}_{2040}$ is $> \tilde{fP}_{2090}$ stems in part from how the seasonality of Great Salt Lake surface temperature responds to atmospheric warming and how this response projects onto lake effect snow.

Dynamically and statistically downscaled climate results indicate warmer temperatures and slightly higher precipitation in 2040s and 2090s (Figure 5). The results indicate a precipitation increase of about 0%–10% and temperature increase in a range of 2°C–6°C by the end of the century. The projected climate results are consistent with other studies such as the climate projection for the Rocky Mountain headwaters of Colorado River (Christensen et al. 2004; Ray et al. 2008). The results of these downscaled climate projections in the State of Utah and the Jordan River basin are also reported in other studies (Scalzitti et al. 2016a, b; Strong et al. 2017; Khatri et al. 2018).

Impact of Climate Change at the Big Cottonwood Site

Figure 6 presents simulated mean daily streamflow and sediment load at the mouth of Big Cottonwood Creek for 2000s, 2040s, and 2090s using data from the dynamically downscaled WRF model for RCP6.0 climate scenario. The mean daily streamflow characteristics are projected to be changed in 2040s and 2090s compared to 2000s (Table 2). The percentage increase of the annual streamflow in 2040s and 2090s compared to 2000s will be about 11.2% and 6.8%, respectively. The timing of the 50th percentile of the cumulative annual streamflows are projected to be shifted about four weeks earlier in 2040s (on April 25) and nearly eight weeks in 2090s (on March 18) compared to 2000s (on May 28).

Figure 6b shows simulated sediment load and its timing in 2040s and 2090s. The mean daily sediment load in 2000s was 1.3 t/day 1.4 t/day in 2040s and 1.8 t/day in 2090s (Table 2). Those changes in the sediment concentration in the near and far future will lead to increases in the mean annual sediment load by 6.7% and 39.7% in 2040s and 2090s. The 50th percentile of the annual sediment load was observed on May 31 in the 2000s. This timing is projected to be shifted earlier by four weeks in the 2040s (on April 23) and about seven weeks in the 2090s (on March 20).

Uncertainty in Impact of Climate Change at the Big Cottonwood Site

Figure 7 presents the range of mean daily streamflow and sediment load in 2040s and 2090s stemming from climate uncertainty. The range of mean streamflow uncertainty in 2040s, due to minimum and maximum climate scenarios will be 1.8 and 2.1 m^3/s, respectively (Table 2 and Figure 7a). Similarly, the net annual volume changes are projected to be (−23.3%) and (+16.5%) compared to RCP6.0. The total uncertainty in the timing of the 50th percentile of

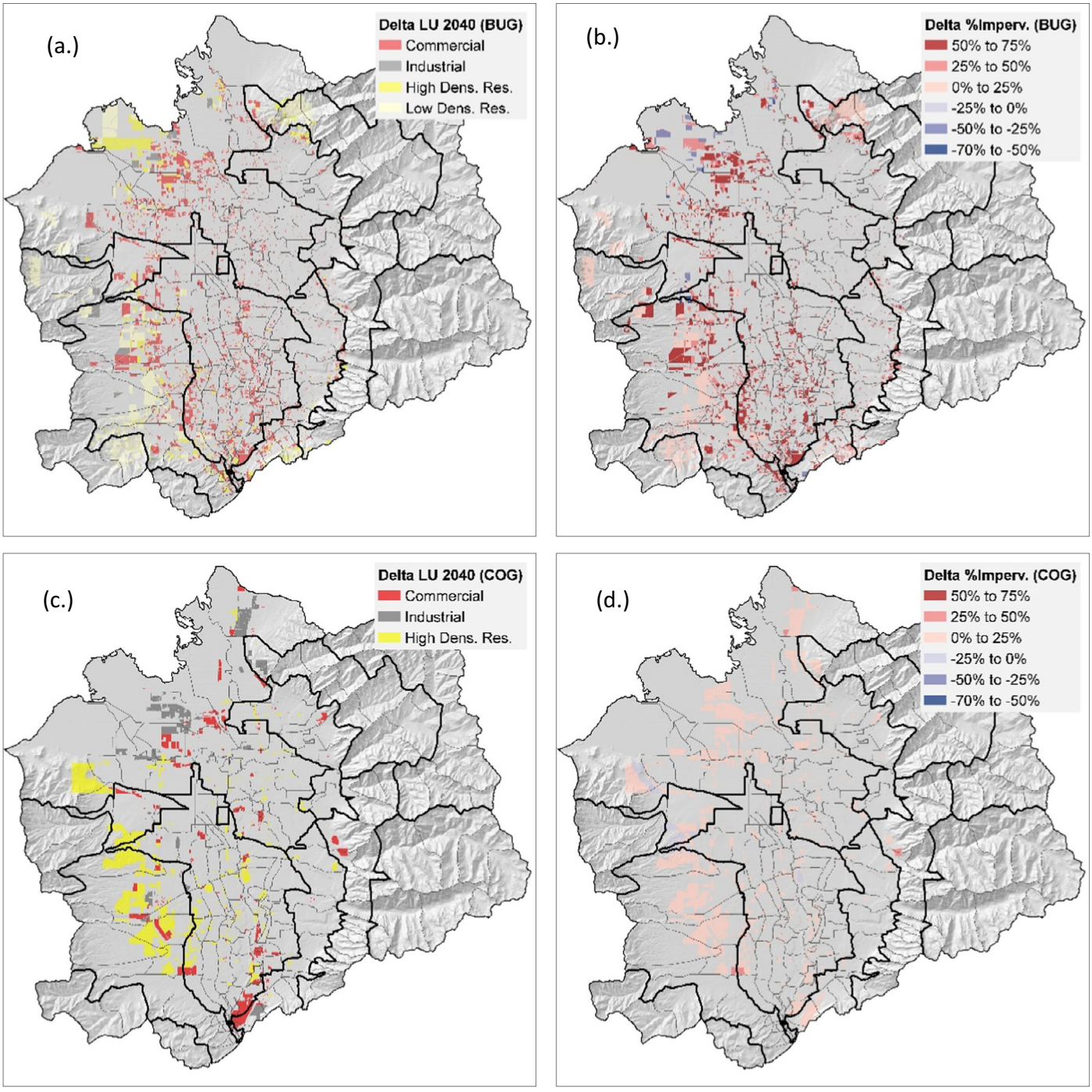

FIGURE 4. Modeled land use (LU) and impervious cover changes using business-as-usual-growth (BUG) scenario (a,b) and centers-oriented-growth (COG) scenario (c,d).

mean annual streamflow, due to the climate uncertainty, will be in a range of three weeks (i.e., min: on May 17, WRF-based RCP 6.0: on April 25, and max: on April 17). Similarly, there was not significant uncertainty on the mean streamflow in 2090s (2.0–2.6) m^3/sec (Figure 7c). The resulting uncertainty in the mean annual streamflows are estimated about (−16.6%) and (+16.5%). The total temporal uncertainty in the timing of the 50th percentile of the annual streamflow will be about three weeks (on May 17, on April 26, and on April 17).

The characteristics of the sediment concentrations in 2040s follow similar trends of the streamflow (Table 2 and Figure 7b). The total uncertainty on the

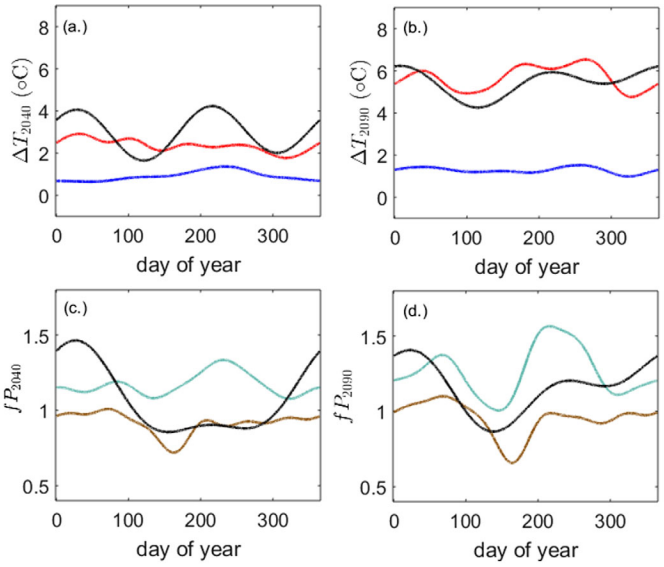

FIGURE 5. (a) Future changes in temperature for 2035–2044 (ΔT_{2040}). The red and blue curves are the upper and lower quartiles of the statistically downscaled ensemble for the Jordan River basin, and the black curve is the average across the eight weather station locations in the dynamically downscaled RCP6.0 scenario. (b) Same as (a), but for 2085–2094 change factors (ΔT_{2090}). (c,d) Same as (a, b) but for precipitation change factors (fP_{2040} and fP_{2090}), and the upper and lower quartiles for the statistically downscaled data are green and brown. RCP, Representative Concentration Pathway.

mean annual sediment load due to the climate scenarios compared to WRF-based RCP 6.0 are (−32.5%) and (+23.2%). The total uncertainty on the timing of the 50th percentile of the sediment load will be about three weeks. Similarly, the mean annual uncertainty on the sediment load due to climate change in 2090s will be in a range of (−38.3%) and (+23.6%) (Figure 7d). The total uncertainty in the timing of the annual 50th percentile sediment flow is projected around five weeks.

Impact of Climate Change and LULC Change at the Jordan River Site

The Jordan River site was evaluated for sensitivity to climate and LULC change scenarios. The results presented at this site include: (1) analysis of the most influential LULC change scenario, (2) sensitivity analysis, and (3) projected impact analysis.

Sensitivity of LULC Change Scenarios. The most sensitive LULC scenario out of three LULC scenarios (i.e., continuation of the existing LULC, BUG, and COG) was evaluated using a consistent climate input (i.e., the dynamically downscaled RCP6.0 scenario) for 2040s. The sensitivity results showed the mean daily streamflow characteristics generated by each of the three LULC change scenarios were not significantly different (Table 3 and Figure 8). The percentage of annual streamflow changes based on the BUG and COG LULC scenarios compared to the existing LULC were (+0.1%) and (+2.7%), respectively (Figure 8a). The timing of the 50th percentile of annual streamflow observed from the corresponding three scenarios were within a three-day period of June 8. Similarly, the results of the sediment load were not significantly different for the three LULC scenarios (Table 3 and Figure 8b). The timing of the 50th percentile of annual sediment load resulting from the corresponding three LULC scenarios were within a one-week period of April 14.

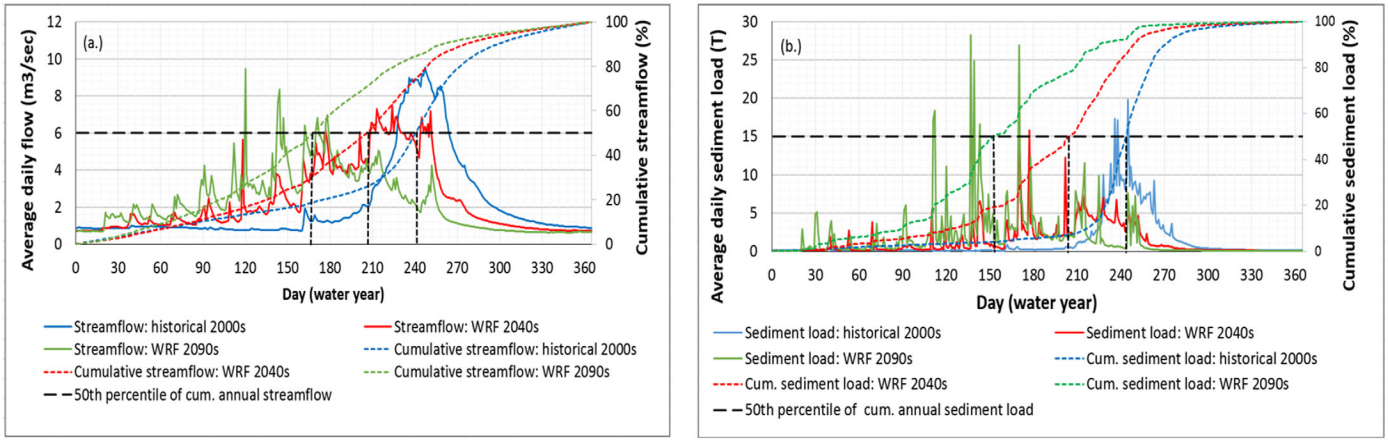

FIGURE 6. (a) Simulated mean daily streamflow based on the dynamically downscaled RCP6.0 climate scenario (denoted Weather Research and Forecasting [WRF] in caption), cumulative annual volume of the streamflow, and timing of the 50th percentile of cumulative annual flow in 2000s, 2040s, and 2090s at the Big Cottonwood Canyon mouth. (b) Similar analysis for the sediment load in tons (T).

TABLE 2. Streamflow and sediment concentration for Big Cottonwood Creek at Canyon Mouth.

Climate change scenarios/parameters	Historical 2000s	Minimum 2040s	Minimum 2090s	RCP6 2040s	RCP6 2090s	Maximum 2090s	Maximum 2090s
A) Streamflow (m^3/s)							
Mean	2.1	1.8	2.0	2.4	2.3	2.1	2.6
Minimum	0.7	0.6	0.7	0.7	0.6	0.6	0.7
Maximum	9.5	8.2	8.7	7.5	9.4	9.0	9.3
Standard deviation	2.1	1.9	2.0	1.9	1.6	2.0	2.2
B) Sediment concentration (mg/L)							
Mean	3.4	3.3	3.4	4.5	6.2	5.0	6.3
Minimum	1.5	1.5	1.5	1.5	1.4	1.5	1.6
Maximum	24.9	47.0	33.4	41.5	106.7	62.6	60.4
Standard deviation	3.5	3.9	3.8	4.7	9.5	6.9	8.2

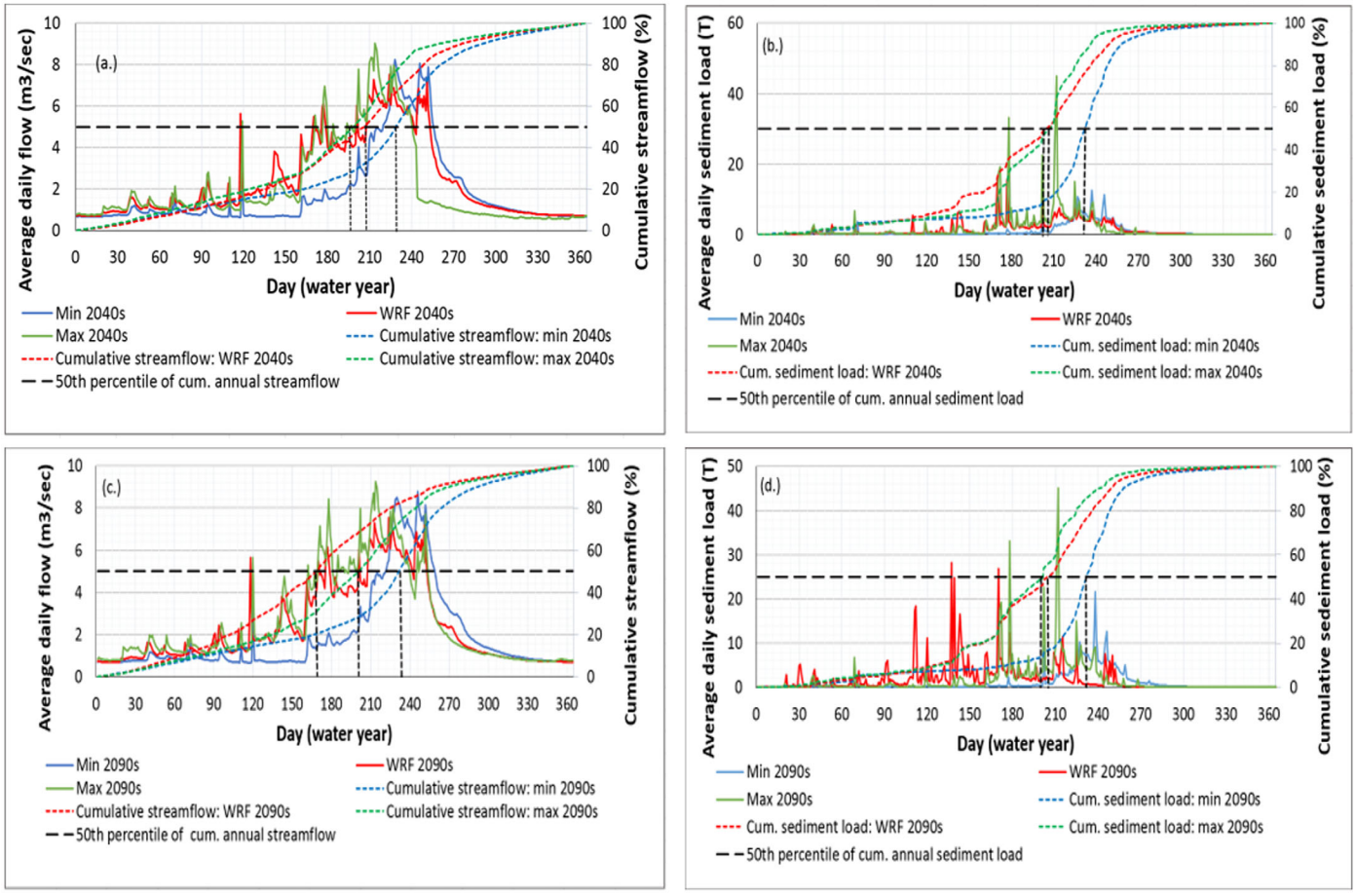

FIGURE 7. (a,c) Uncertainty in mean daily streamflow due to three climate change and LULC, scenarios, cumulative annual volume of the streamflow, and timing of the 50th percentile of annual flow for 2040s and 2090s at the Big Cottonwood Canyon mouth. (b,d) Similar analysis for the sediment load (*T*).

Sensitivity of Streamflow and Sediment Load with Climate and LULC Change. The objective of the sensitivity analysis in this case was to determine the relative impact of the climate and LULC change to the streamflow and sediment concentration. The sensitivity results of the daily streamflow and sediment load showed that the climate change driver is more critical than LULC change (Table 3 and Figure 9a). The timing of the 50th percentile flow for the three scenarios were May 30, April 8, and April 10.

TABLE 3. Sensitivity analysis at the Jordan River above Surplus Canal.

	Sensitivity to LULC change only			Sensitivity to LULC and climate change		
Change scenarios/parameters	**Existing LULC: 2000s**	**BUG: 2040s**	**COG: 2040s**	**BUG in 2040s & historical climate 2000s**	**Existing LULC & future climate RCP6**	**BUG in 2040s & future climate RCP6**
A) Streamflow (m^3/s)						
Mean	15.1	16.2	15.8	13.7	15.8	16.2
Minimum	8.1	8.1	8.1	6.8	8.1	8.1
Maximum	30.6	32.1	30.8	33.0	30.6	32.1
Standard deviation	5.8	6.0	5.9	5.7	5.9	6.1
B) Sediment concentration (mg/L)						
Mean	27.6	28.2	27.3	28.5	27.6	28.2
Minimum	0.6	0.6	0.5	2.7	0.6	0.6
Maximum	91.9	81.0	80.0	66.6	91.9	81.0
Standard deviation	15.7	15.4	15.2	17.8	15.7	15.4

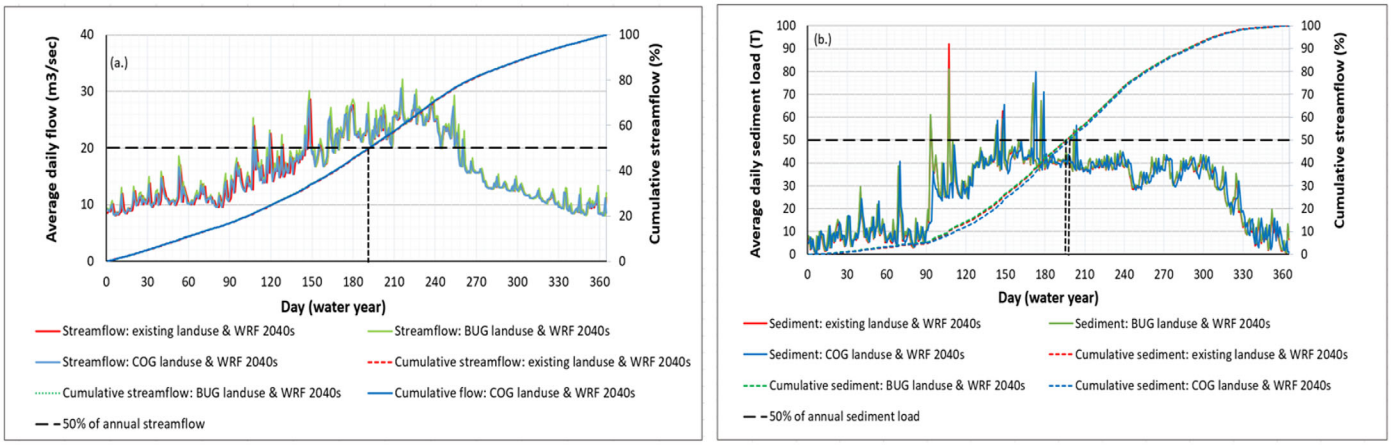

FIGURE 8. (a) Sensitivity of streamflow and (b) sediment load to three LULC changes scenarios under a consistent climate scenario (dynamically downscaled RCP6.0; denoted WRF in caption) in the Jordan River.

The mean annual volume change on scenarios (2) and (3) with reference to (1) were 15.4% and 18.5%.

The results of sediment sensitivity show similar trends of the hydrograph (Table 3 and Figure 9b). The total increase in the annual sediment load based on scenarios (2) and (3) compared to scenario (1) was 10.2% and 14.4%. The simulated timings of the 50th percentile of the sediment load for scenarios (1), (2), and (3) were within a three-week time period (May 9, April 10, and April 8).

Impact of Climate and LULC Change. The results of the impact of the climate (dynamically downscaled RCP 6.0 scenario) and LULC change (BUG scenario) on streamflow and sediment load in 2040s and 2090s are presented in Table 4 and Figure 10. The total increases in mean annual streamflow in 2040s and 2090s compared to 2000s were 14.5% and 15.3%. The timing of the 50th percentile of annual streamflow, in 2000s, was observed in the second week of May (on May 11), whereas the corresponding timings for the 2040s and 2090s will shift earlier to April 10 and March 3, respectively (Figure 10a). The annual increase in sediment load in 2040s and 2090s compared to 2000s are projected to be 7.4% and 14.2%, respectively (Table 4 and Figure 10b). The timing of the 50th percentile of the annual sediment load in 2040s (on April 15) and 2090s (on April 6) will be about five and six weeks earlier compared to 2000s (on June 10).

Uncertainty in Impact of Climate Change and LULC Change. The uncertainty in impact of LULC change was simulated considering three climate scenarios and the BUG LULC change scenario (Table 4 and Figure 11) The uncertainties to the mean annual streamflow will be in a range of (−10.2%) to (+1.5%) and about one week to the 50th percentile timing of the mean annual streamflow in 2040s (Figure 11a). Similarly, the mean daily 2090s streamflow will be

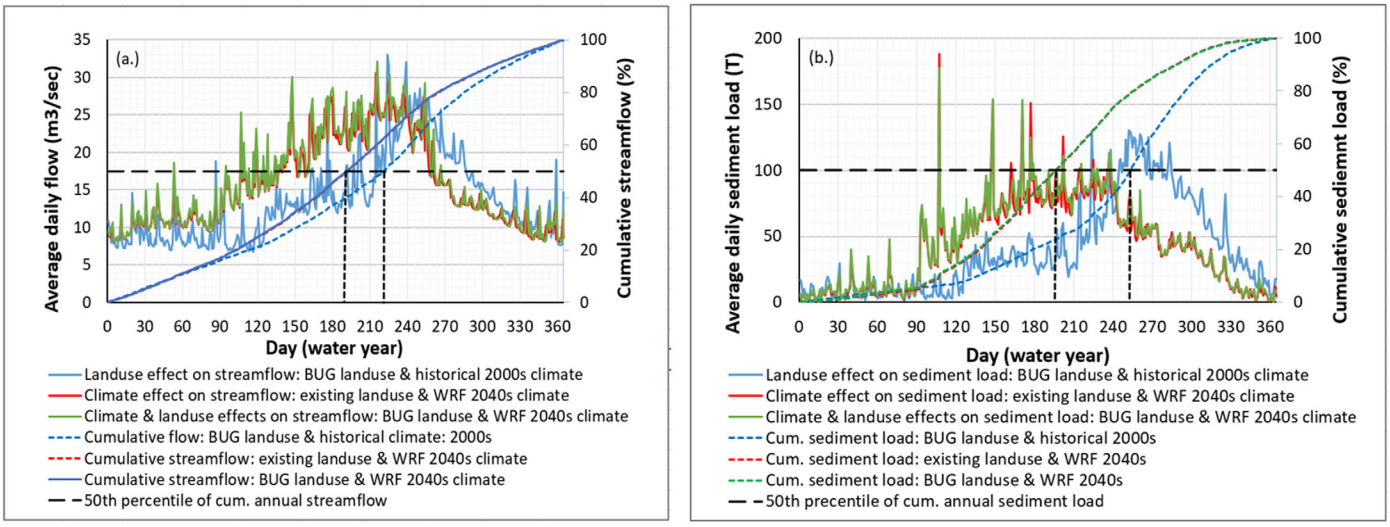

FIGURE 9. (a) Sensitivity of Jordan River streamflow to LULC changes and climate change (dynamically downscaled RCP6.0 scenario in 2040s; denoted WRF in caption), and (b) similar analysis for sediment load.

TABLE 4. Streamflow and sediment concentration for Jordan River above Surplus Canal.

Climate change scenarios/parameters	Historical 2000s	Minimum		RCP6		Maximum	
		2040s	2090s	2040s	2090s	2040s	2090s
A) Streamflow (m^3/s)							
Mean	13.8	14.1	14.7	15.8	15.9	15.5	15.9
Minimum	6.8	7.8	8.1	8.0	8.1	7.9	8.1
Maximum	32.8	27.8	30.3	30.6	32.7	36.3	32.8
Standard deviation	6.0	5.0	5.2	5.9	5.3	6.0	5.3
B) Sediment concentration (mg/L)							
Mean	28.7	28.8	28.2	27.6	29.70	29.1	29.3
Minimum	1.4	0.6	0.6	0.6	0.5	0.7	0.8
Maximum	72.8	62.7	62.2	91.9	160.6	95.4	99.9
Standard deviation	18.2	16.4	16.0	15.7	18.8	16.8	16.9

14.7 and 16.2 m^3/s, with corresponding uncertainty of (−7.6%) and (+2.1%) (Figure 11c). The uncertainty in the timing of the 50th percentile of streamflow is about four weeks.

The uncertainty in daily mean value of the sediment concentration for the minimum and maximum climate change scenarios compared to the RCP6.0 (43.5 t/day) will be (−8.3%) and (+3.9%) (Table 4 and Figure11b). The timing of the annual 50^{th} percentile of sediment load is within a two-week range. The uncertainties on sediment load and timing in 2090s are projected to be (−11.5%) to (+3.6%) and about two weeks, respectively.

Relationship between Streamflow and Sediment Load

Figure 12 presents the relationship between streamflow and sediment concentration at the Canyon Mouth in Big Cottonwood Creek and above the Surplus Canal station in Jordan River in 2040s and 2090s. The streamflows and sediment concentration data considered for the analysis include the model results of the three climate change scenarios and BUG LULC change for 2040s and 2090s. The regression results show nonlinear relationships between the streamflow and sediment concentration.

The uncertainty in seasonal streamflow and sediment load at the two stations are presented using box plots (Figure 13). The minimum and maximum values in the plots represent 95% confidence intervals. The results show decadal and seasonal variability in the streamflows and sediment in 2000s, 2040s, and 2090s. As shown, the results of the streamflows and sediment shifted the seasonality in 2040s and 2090s compared to the 2000s results.

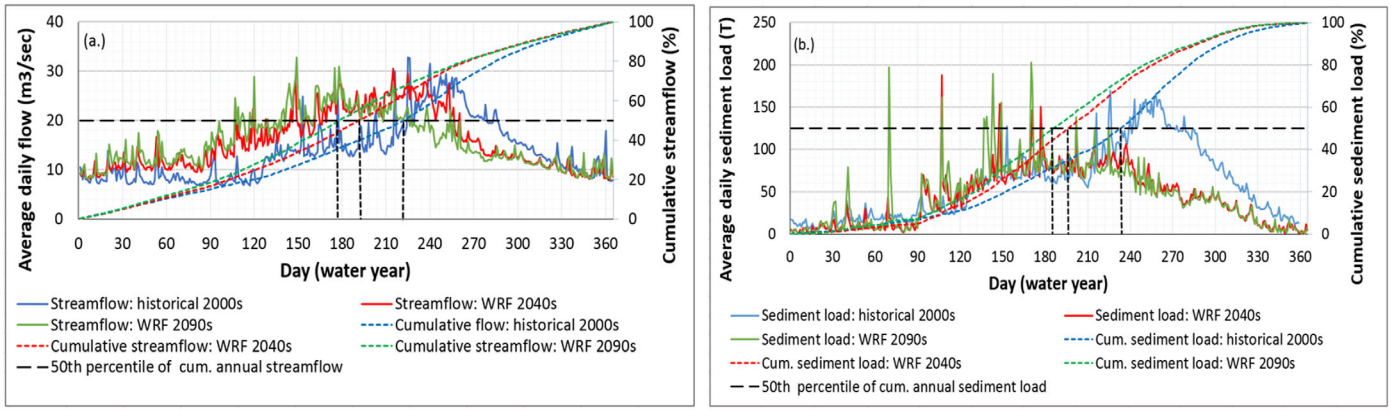

FIGURE 10. (a) Simulated mean daily streamflow based on dynamically downscaled RCP6.0 climate scenario (denoted WRF in caption), corresponding cumulative volume of the annual streamflow, and timing of the 50th percentile of the annual streamflow for 2000s, 2040s, and 2090s in the Jordan River. (b) Similar analysis for sediment load (T).

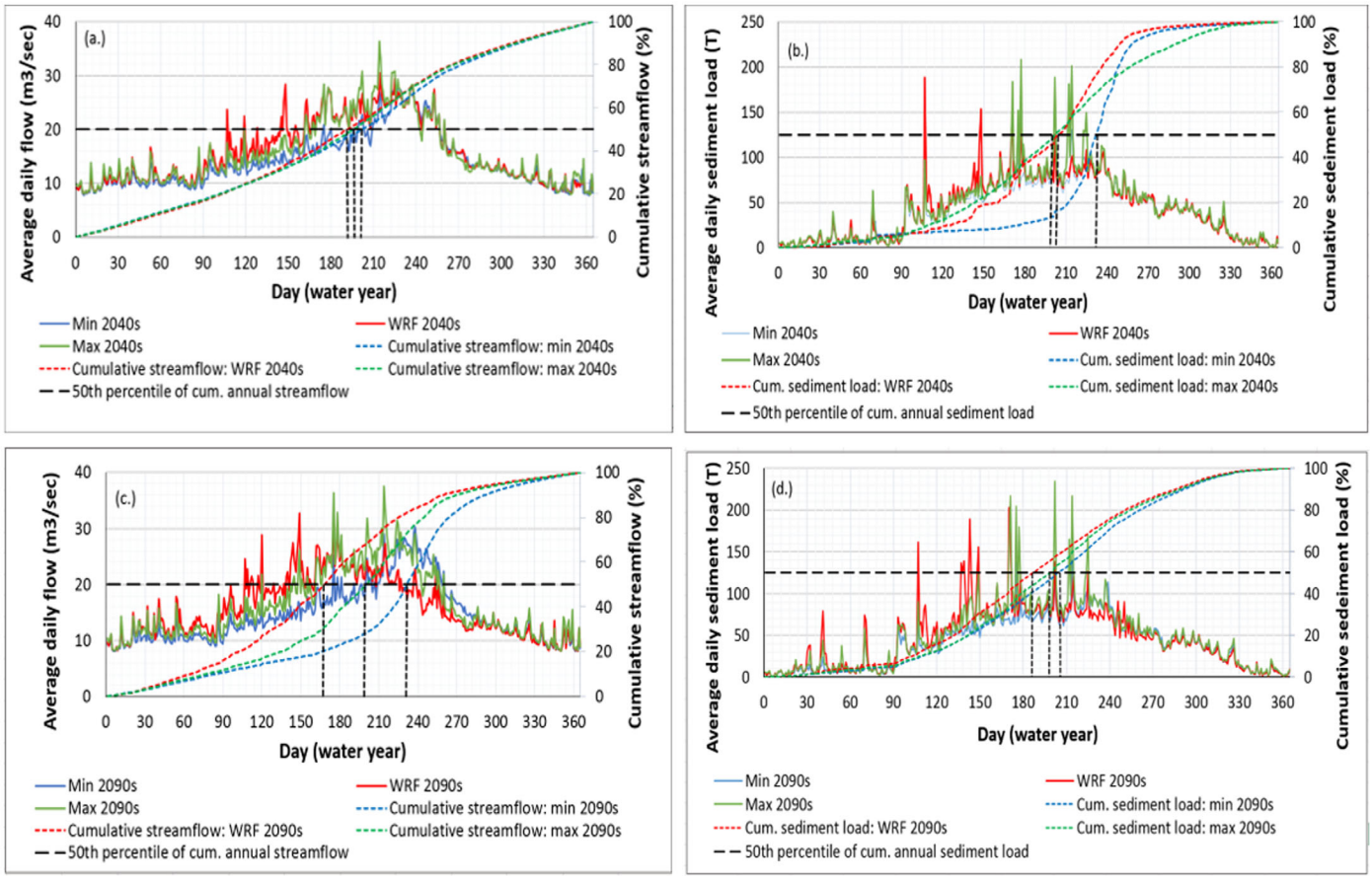

FIGURE 11. Uncertainty in mean daily streamflow and sediment load due to three climate change scenarios for 2040s (a,b) and 2090s (c,d) in the Jordan River.

DISCUSSION

Projected Future Streamflow

The upper Big Cottonwood subwatershed is not anticipated to undergo significant increased urbanization and human intervention. Therefore, the future results presented on streamflow and sediment load in the upper Big Cottonwood subwatershed has a negligible effect of LULC change and are exclusively due to the impact of climate change.

The predicted increase in streamflow was mainly due to a projected slight increase in precipitation in

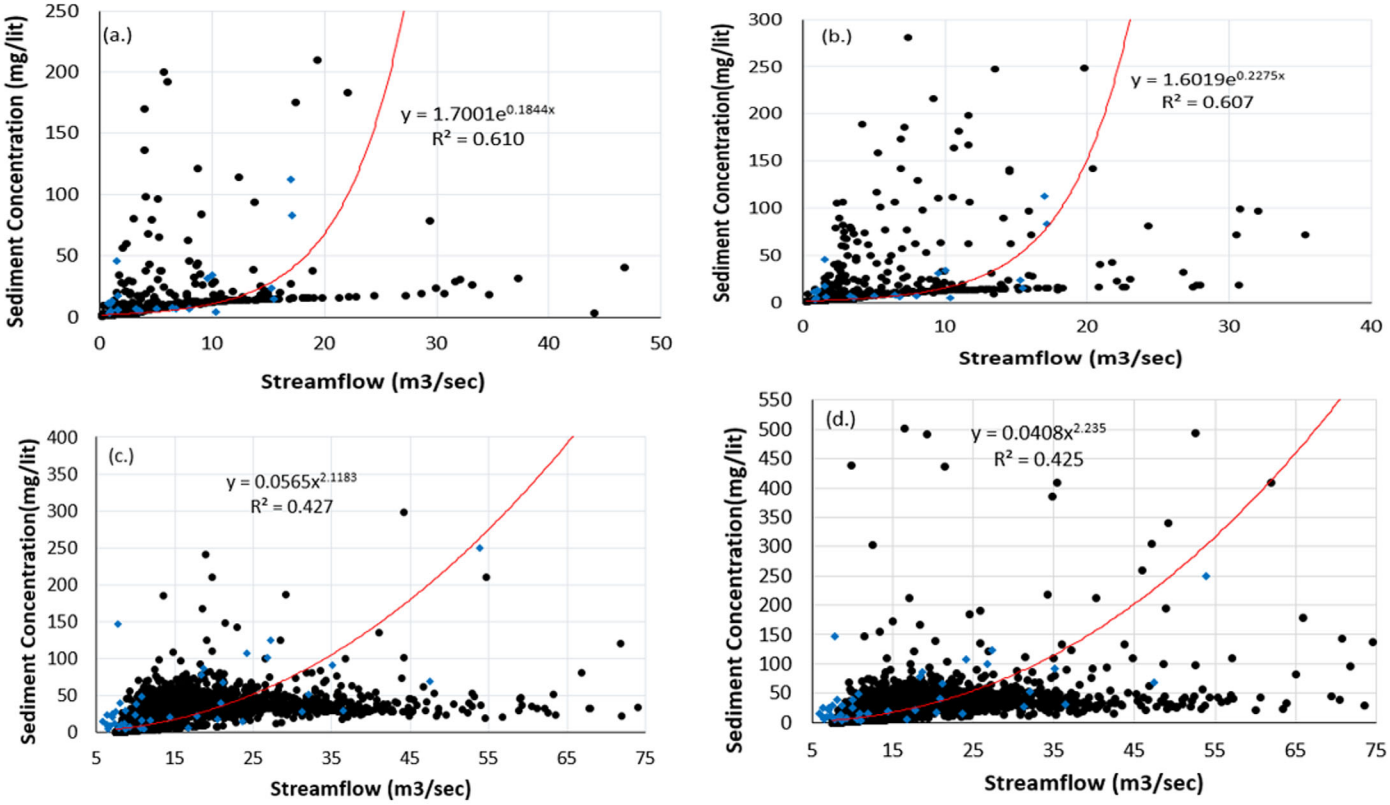

FIGURE 12. (a,b) Regression results for streamflow and sediment concentration at the Canyon Mouth in Big Cottonwood Creek in 2040s and 2090s and (c,d) the same relations in the Jordan River above the Surplus Canal. Blue filled circles represent the historical observations data used for the model calibration, and black filled circles indicate simulation results. Regression formulation and associated R^2 are indicated on each panel.

2040s and 2090s under the dynamically downscaled RCP6.0 scenario. Although beyond the scope of this study, potential future shifts in vegetation and growing season in the mountainous areas could result in increased evapotranspiration that somewhat or entirely offsets the predicted future increase in precipitation. Mahat and Tarboton (2012) coupled results from a physically based energy balance model with observations over multiple seasons and concluded that forest areas collected 10%–20% less snow than adjacent open areas. The range of uncertainty in the streamflow at the Jordan River site compared to Big Cottonwood stems in part from the variability of the subcatchment in the Jordan River (mainly urbanized land uses), effects of the inflows from Utah Lake, and other human interventions (e.g., irrigation diversion, wastewater effluent).

The results of this study are consistent with other studies (e.g., Christensen et al. 2004; Barnett et al. 2005; Clow 2010) indicating substantial variability in streamflow related to the uncertainty in precipitation and the timing of snowmelt. Christensen et al. (2004) suggested an annual runoff decrease in Colorado River basin by about 10% in the middle of the century (2040–2069) for the business as usual climate change scenario. Ray et al. (2008) showed decreases in runoff ranging from 6% to 20% by 2050 compared to the 20th Century average based on the multimodel average projections for the Upper Colorado River Basin. Chase et al. (2016) found mean annual streamflows projected to increase (11%–21%) for Middle Musselshell River and Cottonwood Creek in Montana for years 2021–2038, 2046–2063, and 2071–2088.

The percentile of mean annual streamflow volume occurred three to five weeks earlier. The earlier timing of snowmelt runoff was also reported in other studies. For example, Clow (2010) showed a two to three week earlier shift in the high mountains of the Colorado region; Stewart et al. (2005) found advancement of about 15–20 days in the western U.S. The escalated timing of the snowmelt-dominated streamflow is due to change in the extent and timing of the annual snowpack (i.e., later snowpack initiations and earlier snowpack disappearance), change in the length of the snow-covered season, snowmelt periods at lower elevations during the winter, and increasing springtime air temperatures (Stewart et al. 2005; Clow 2010; Harpold et al. 2012).

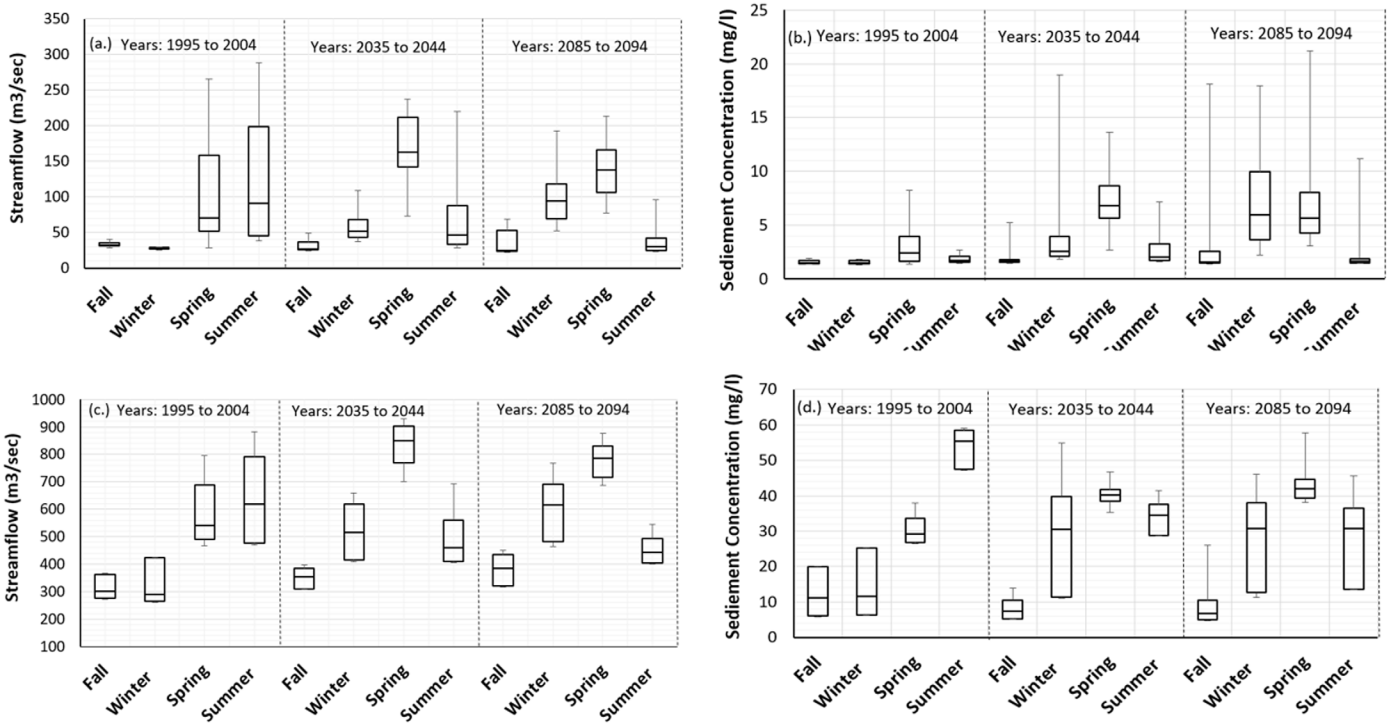

FIGURE 13. Box plots showing the 5th percentile, first quartile, median, third quartile, and 95th percentile of seasonal streamflow and sediment concentration in 2000s, 2040s, and 2090s based on dynamically downscaled RCP6.0 climate scenario at the mouth of Big Cottonwood Creek (a,b), and above the Surplus Canal in the Jordan River (c,d), respectively.

Climatological and hydrological modeling in mountain environments is challenging due to pronounced spatial and temporal heterogeneity and complex orographic precipitation and snowfall processes which are not sufficiently understood or represented in the models (Kapnick and Hall 2012; Burke and Ficklin 2017). The uncertainty in streamflow trends are the result of interactions between multiple factors including reduced snow accumulations and increased late season melt rates associated with warming temperatures (Wang et al. 2011). The relative impacts of these two factors are found to be strongly influenced by the seasonal variations of temperature, precipitation magnitudes, snow-to-rain ratios, and the temporal distribution of snow and rain events. In this case, the reported positive changes are based on the dynamically downscaled RCP 6.0 scenario, and climate uncertainty may result in larger or smaller changes in the magnitude and timing of streamflow.

Projected Future Sediment Load

Our study projected the mean daily sediment load at the Big Cottonwood Creek site to increase 1.4 tons/day (≈3.8 t/km^2/yr) in 2040s to 1.7 t/day (≈4.9 tons/km^2/yr) in 2090s. The predicted sediment yields per watershed area are consistent with the results reported by Allmendinger et al. (2007), which vary from 0.2 t/km^2/yr in the Colorado River to 6.3×10^3 tons/km^2/yr in Tributary at Gwynns Falls, Maryland. The predicted increase in sediment yield has implications for river and floodplain managers, as increased maintenance of waterways will be required in areas prone to deposition.

The significant increase in sediment load from the Big Cottonwood Canyon stems in part from an increased fraction of rain vs. snow, and more frequent and higher-intensity rainfall events intercepted by a steeply sloped watershed. Although the Jordan River site has a large catchment area, the relative increase in the sediment load was less pronounced in the future. This could be due to the presence of several canal diversions upstream of the Jordan site and the effects of Utah Lake management at the upstream boundary. Moreover, the Jordan River passes through urban areas, where a reduction in sediment supply and an increase in flood discharge will generally lead to channel enlargement and the removal of transportable sediment in the long term.

Sensitivity of Streamflow and Sediment Load

The findings that all three LULC scenarios have nearly equal impacts on the streamflows and

sediment load at the Jordan River site could be due to the presence of fully developed areas (impervious areas) upstream of the gage site. The results showed the streamflows and sediment load at the Jordan River site are more sensitive to future climate change compared to LULC change (Figure 9a and 9b).

The reasons for the dominance of climate impact on streamflow and sediment load include limited opportunities for impervious area growth in the valley and pre-dominance of inflows from the snow-dominated mountainous watershed. However, the magnitude of change would be different in other gaged sites in the Jordan River where increases in developed lands represent a larger percentage of watershed area. It is also noted that streamflow and sediment load for the Jordan River at Surplus Canal are primarily driven by runoff from the mountains and outflow from Utah Lake, and does not include sediment associated with channel enlargement. In addition, the expected future increased urbanization of Utah Valley could significantly impact the discharge and sediment load from Utah Lake.

Relationship between Streamflow and Sediment Load

The regression results of the streamflow and sedimentation at both sites showed a nonlinear relationship (Figure 12). It is evident that variability in the sediment load in a watershed depends on the erosion rates, delivery of eroded sediments to streams, drains and other pathways, and subsequent instream transport, scour, and deposition processes (Donigian 2002). The erosion process is strongly and nonlinearly affected by the higher percentiles of rainfall intensity and magnitude. The hydrological processes are modified with urbanization and human interventions. Both the climate and LULC change drivers are of dynamic nature. As a result, the sediment yield rate resulting from the change in erosion rates in response to climate perturbations can be highly nonlinear and catchment specific (Coulthard et al. 2012; Nunes et al. 2013). Similar types of nonlinear regressions were reported in other studies (Haan et al. 1994; Donigian and Love 2003; Mullan 2013).

The trends of seasonal changes in streamflow and sediment are similar at both the sites but with a higher degree of uncertainty at the Jordan River site (Figure 13). This could be due to the effect of the inflows from Utah Lake. The results of the seasonal variability are consistent with earlier studies in the Western U.S. (e.g., Barnett et al. 2005) which also showed that the spring streamflow maximum will occur about one month earlier by 2050. This shift in timing has significant implications for water suppliers, as less water is projected to be stored in snowpack and for a shorter period of time.

Sediment erosion in HSPF uses a method that is similar to the USLE, which uses a sediment-detachment approach coupled with transport capacity based on overland flow. On pervious land areas, the erosion process is represented as the net result of detachment of soil particles by raindrop impact on the land surface and then subsequent transport of these particles by overland flow. On impervious surfaces, soil splashes by raindrop impact are neglected and solids wash off is often controlled by the rate of accumulation of soil materials. Thus, rainfall is critical to the detachment and the removal involved in erosional processes on the land surface, and finally sediment delivery from the landscape and instream transport, all of which are very uncertain processes. However, with the predicted future increase in rainfall intensity of storms, and more frequent rain vs. snow events, it is anticipated that the erosion and sediment yield from the landscape will increase.

CONCLUSIONS

Our results show that the mean daily streamflow at the canyon mouth of Big Cottonwood Creek driven by the dynamically downscaled RCP6.0 climate scenario are projected to increase by about 11.2% (with uncertainty of [−23.3%] to [+16.5%]) in the 2040s and about 6.8% (with uncertainty of [−16.6%] to [+16.5%]) in the 2090s as compared to the historical records of the 2000s. The corresponding increases in sediment load in the same period are expected to be about 6.7% (with uncertainty of [−32.5%] to [+23.2%]) and 39.7% (with uncertainty of [−38.3%] to [+23.6%]), respectively. Similarly, the total increase in mean annual streamflow above the Surplus Canal in the Jordan River will reach 14.5% (with uncertainty of [−10.2%] to [+1.5%]) and 15.3% (with uncertainty of [−7.6%] to [+2.1%]) and sediment load will increase 7.4% (with uncertainty of [−8.3%] to [+3.9%]) and 14.2% (with uncertainty of [−11.5%] to [+3.6%]) in the 2040s and 2090s, respectively.

The shift toward earlier timing of the 50th percentile of the mean annual flow is expected to reach about four weeks in the 2040s and eight weeks in 2090s, with an uncertainty of four and two weeks depending on climate scenario, respectively. Our results suggest that the range of possible future streamflows and sediment loads in the Jordan River watershed is primarily driven by future climate change, whereas the changes in LULC play a

secondary role. It should be noted that the impact of warming climate and increased precipitation may induce seasonal shifts that could alter patterns of streamflow and sediment loading. The early shift in the timing of the 50th percentile in the streamflow and sediment loading is driven by changes in precipitation, snowpack, and snowmelt, with a nonlinear relationship between streamflow and the sediment load.

The approach used here represents a plausible range of scenarios but does not capture all possible future conditions. The hourly input of the dynamically downscaled meteorological data provided high temporal and spatial resolutions, but did not necessarily capture climate and weather extremes which may be underrepresented in the CMIP5. In addition, modifications to the inflows from Utah Lake, diversions to irrigation canals from the Jordan River, diversions for potable water supply from the tributaries, application of the urban and agricultural best management practices, and other new development not taken into account in this study may have significant effects on the predicted streamflow and sediment load. Additional unevaluated factors potentially impacting streamflow and sediment yield include increased frequency of forest fires, changes in the composition of vegetated cover, winter road management practices (i.e., sand application), and stormwater management practices in the urbanized area. Additionally, the HSPF model is a semi-lumped model and considerably large areas are used for the modeling and subsequent analysis. Therefore, future studies may benefit from further subzoning of LULC.

ACKNOWLEDGMENTS

This work was supported by the National Science Foundation cooperative agreement EPSCoR EPS-1208732. Any opinions, findings, and conclusions or recommendations expressed in this material are those of the authors and do not necessarily reflect the views of the National Science Foundation and affiliated institutions of the authors. We would like to acknowledge high-performance computing support from Yellowstone (award UUSL006) provided by NCAR's Computational and Information Systems Laboratory, sponsored by the National Science Foundation, as well as from the University of Utah Center for High Performance Computing (CHPC). We would also like to acknowledge the support from Bryan Close (Eng. staff at Stantec Consulting Inc.) and Salt Lake County Office Utah for sharing the HSPF model and report.

LITERATURE CITED

Ahearn, D.S., R.W. Sheibley, R.A. Dahlgren, M. Anderson, J. Johnson, and K.W. Tate. 2005. "Land Use and Land Cover Influence on Water Quality in the Last Free-Flowing River Draining the Western Sierra Nevada, California." *Journal of Hydrology* 313 (3): 234–47. https://doi.org/10.1016/j.jhydrol.2005.02.038.

Al-Abed, N.A., and H.R. Whiteley. 2002. "Calibration of the Hydrological Simulation Program Fortran (HSPF) Model Using Automatic Calibration and Geographical Information Systems." *Hydrological processes* 16 (16): 3169–88. https://doi.org/10.1002/hyp.1094.

Allan, D., D. Erickson, and J. Fay. 1997. "The Influence of Catchment Land Use on Stream Integrity across Multiple Spatial Scales." *Freshwater Biology* 37 (1): 149–61. https://doi.org/10.1046/j.1365-2427.1997.d01-546.x.

Allmendinger, N.E., J.E. Pizzuto, G.E. Moglen, and M. Lewicki. 2007. "A Sediment Budget for an Urbanizing Watershed, 1951–1996, Montgomery County, Maryland, USA." *Journal of the American Water Resources Association* 43 (6): 1483–98. https://doi.org/10.1111/j.1752-1688.2007.00122.x.

Arnell, N.W., and B. Lloyd-Hughes. 2014. "The Global-Scale Impacts of Climate Change on Water Resources and Flooding under New Climate and Socio-Economic Scenarios." *Climatic Change* 122 (1–2): 127–40. https://doi.org/10.1007/s10584-013-0948-4.

Arnold, J.G., D.N. Moriasi, P.W. Gassman, K.C. Abbaspour, M.J. White, R. Srinivasan, C. Santhi, R. Harmel, A. Van Griensven, and M.W. Van Liew. 2012. "SWAT: Model Use, Calibration, and Validation." *Transactions of the American Society of Agricultural and Biological Engineers* 55 (4): 1491–508. https://doi.org/10.13031/2013.42256.

ASCE (ASCE Task Committee on Definition of Criteria for Evaluation of Watershed Models of the Watershed Management Committee, Irrigation, and Drainage Division). 1993. "Criteria for Evaluation of Watershed Models." *Journal of Irrigation and Drainage Engineering* 119 (3): 429–442. https://doi.org/10.1061/(ASCE)0733-9437(1993)119:3(429).

Baker, A. 2005. "Land Use and Water Quality." *Encyclopedia of Hydrological Sciences*. https://doi.org/10.1002/0470848944.hsa195.

Bardsley, T., A. Wood, M. Hobbins, T. Kirkham, L. Briefer, J. Niermeyer, and S. Burian. 2013. "Planning for an Uncertain Future: Climate Change Sensitivity Assessment Toward Adaptation Planning for Public Water Supply." *Earth Interactions* 17 (23): 1–26. https://doi.org/10.1175/2012EI000501.1.

Barnett, T.P., J.C. Adam, and D.P. Lettenmaier. 2005. "Potential Impacts of a Warming Climate on Water Availability in Snow-Dominated Regions." *Nature* 438 (7066): 303. https://doi.org/10.1038/nature04141.

Benavidez, R., B. Jackson, D. Maxwell, and K. Norton. 2018. "A Review of the (Revised) Universal Soil Loss Equation ((R) USLE): With a View to Increasing Its Global Applicability and Improving Soil Loss Estimates." *Hydrology and Earth System Sciences* 22 (11): 6059–86. https://doi.org/10.5194/hess-22-6059-2018.

Bicknell, B.R., J.C. Imhoff, J.L. Jr Kittle, T.H. Jobes, A.S. Donigian, Jr., and R. Johanson. 2001. Hydrological Simulation Program — Fortran (HSPF), User's Manual for Release 12." U.S.EPA National Exposure Research Laboratory, Athens, GA, in cooperation with U.S. Geological Survey, Water Resources Division, Reston, VA. https://www.epa.gov/environmental-topics/water-topics.

Birkinshaw, S., and J. Bathurst. 2006. "Model Study of the Relationship between Sediment Yield and River Basin Area." *Earth Surface Processes and Landforms* 31 (6): 750–61. https://doi.org/10.1002/esp.1291.

Borah, D.K., and M. Bera 2004. "Watershed-Scale Hydrologic and Nonpoint-Source Pollution Models: Review of Applications." *Transactions of the American Society of Agricultural Engineers* 47 (3): 789. https://doi.org/10.1023/B:CLIM.0000013684.13621.1f.

Burbidge, S., T. Knowlton, and A. Matheson. 2007. "Wasatch Choices 2040: A New Paradigm for Public Involvement and Scenario Development in Transportation Planning." *Transportation Research Record: Journal of the Transportation Research Board* 1994: 147–53. https://doi.org/10.3141/1994-19.

Burke, W.D., and D.L. Ficklin. 2017. "Future Projections of Streamflow Magnitude and Timing Differ across Coastal Watersheds of the Western United States." *International Journal of Climatology* 37 (13): 4493–508. https://doi.org/10.1002/joc.5099.

Chang, E.K., Y. Guo, and X. Xia. 2012. "CMIP5 Multimodel Ensemble Projection of Storm Track Change under Global Warming." *Journal of Geophysical Research: Atmospheres* 117 (D23). https://doi.org/10.1029/2012JD018578.

Chase, K.J., A.E. Haj, R.S. Regan, and R.J Viger. 2016. "Potential effects of climate change on streamflow for seven watersheds in eastern and central Montana." *Journal of Hydrology: Regional Studies* 7:69–81.

Christensen, N.S., A.W. Wood, N. Voisin, D.P. Lettenmaier, and R.N. Palmer. 2004. "The Effects of Climate Change on the Hydrology and Water Resources of the Colorado River Basin." *Climatic Change* 62 (1–3): 337–63. https://doi.org/10.1023/B:CLIM.0000013684.13621.1f.

Clow, D.W. 2010. "Changes in the Timing of Snowmelt and Streamflow in Colorado: A Response to Recent Warming." *Journal of climate* 23 (9): 2293–306. https://doi.org/10.1175/2009JCLI2951.1.

Coulthard, T., J. Ramirez, H. Fowler, and V. Glenis. 2012. "Using the UKCP09 Probabilistic Scenarios to Model the Amplified Impact of Climate Change on Drainage Basin Sediment Yield." *Hydrology and Earth System Sciences* 16 (11): 4401. https://doi.org/10.5194/hess-16-4401-2012.

Daggupati, P., N. Pai, S. Ale, K.R. Douglas-Mankin, R.W. Zeckoski, J. Jeong, P.B. Parajuli, D. Saraswat, and M.A. Youssef. 2015. "A Recommended Calibration and Validation Strategy for Hydrologic and Water Quality Models." *Transactions of the American Society of Agricultural and Biological Engineers* 58 (6): 1705–19. https://doi.org/10.13031/trans.58.10712.

Deser, C., R. Knutti, S. Solomon, and A.S. Phillips. 2012. "Communication of the Role of Natural Variability in Future North American Climate." *Nature Climate Change* 2 (11): 775. https://doi.org/10.1038/nclimate1779.

Diaz-Ramirez, J., W. McAnally, and J. Martin. 2011. "Analysis of Hydrological Processes Applying the HSPF Model in Selected Watersheds in Alabama, Mississippi, and Puerto Rico." *Applied Engineering in Agriculture* 27 (6): 937–54. https://doi.org/10.13031/2013.40627.

Donigian, A. 2002. "Watershed Model Calibration and Validation: The HSPF Experience." *Proceedings of the Water Environment Federation* 2002 (8): 44–73. https://www.aquaterra.com/resources/pubs/pdf/donigian-2002a.pdf.

Donigian, A., and J. Love. 2003. "Sediment Calibration Procedures and Guidelines for Watershed Modeling." *Proceedings of the Water Environment Federation* 2003 (4): 728–47. https://www.researchgate.net/publication/233520639.

Duda, P., P. Hummel, A. Donigian, Jr., and J. Imhoff. 2012. "BASINS/HSPF: Model Use, Calibration, and Validation." *Transactions of the American Society of Agricultural and Biological Engineers* 55 (4): 1523–47. https://doi.org/10.13031/2013.42261.

Dudula, J., and T.O. Randhir. 2016. "Modeling the Influence of Climate Change on Watershed Systems: Adaptation through Targeted Practices." *Journal of Hydrology* 541: 703–13. https://doi.org/10.1016/j.jhydrol.2016.07.020.

El-Khoury, A., O. Seidou, D. Lapen, Z. Que, M. Mohammadian, M. Sunohara, and D. Bahram. 2015. "Combined Impacts of Future Climate and Land Use Changes on Discharge, Nitrogen and Phosphorus Loads for a Canadian River Basin." *Journal of Environmental Management* 151: 76–86. https://doi.org/10.1016/j.jenvman.2014.12.012.

Engelmann, C.J., A.D. Ward, A.D. Christy, and E.S. Bair. 2002. "Application of the Basins Database and NPSM Model on a small Ohio Watershed." *Journal of the American Water Resources Association* 38 (1): 289–300. https://doi.org/10.1111/j.1752-1688.2002.tb01552.x.

Ewing, R., and K. Bartholomew. 2009. "Comparing Land Use Forecasting Methods: Expert Panel versus Spatial Interaction Model." *Journal of the American Planning Association* 75 (3): 343–57. https://doi.org/10.1080/01944360902956296.

Ficklin, D., B. Barnhart, J. Knouft, I. Stewart, E. Maurer, S. Letsinger, and G. Whittaker. 2014. "Climate Change and Stream Temperature Projections in the Columbia River Basin: Habitat Implications of Spatial Variation in Hydrologic Drivers." *Hydrology and Earth System Sciences* 18 (12): 4897. https://doi.org/10.5194/hess-18-4897-2014.

Francipane, A., S. Fatichi, V.Y. Ivanov, and L.V. Noto. 2015. "Stochastic Assessment of Climate Impacts on Hydrology and Geomorphology of Semiarid Headwater Basins Using a Physically Based Model." *Journal of Geophysical Research: Earth Surface* 120 (3): 507–33. https://doi.org/10.1002/2014JF003232.

Fregonese Associates. 2015. *Envision Tomorrow*, Portland, OR. http://envisiontomorrow.org.

Gupta, H.V., S. Sorooshian, and P.O. Yapo. 1999. "Status of Automatic Calibration for Hydrologic Models: Comparison with Multilevel Expert Calibration." *Journal of Hydrologic Engineering* 4 (2): 135–43. https://doi.org/10.1061/(ASCE)1084-0699(1999)4:2(135).

Haan, C.T., B.J. Barfield, and J.C. Hayes. 1994. *Design Hydrology and Sedimentology for Small Catchments*. Oxford: Elsevier.

Harmel, R., P. Smith, K. Migliaccio, I. Chaubey, K. Douglas-Mankin, B. Benham, S. Shukla, R. Muñoz-Carpena, and B.J. Robson. 2014. "Evaluating, Interpreting, and Communicating Performance of Hydrologic/Water Quality Models Considering Intended Use: A Review and Recommendations." *Environmental modelling & software* 57: 40–51. https://doi.org/10.1016/j.envsoft.2014.02.013.

Harpold, A., P. Brooks, S. Rajagopal, I. Heidbuchel, A. Jardine, and C. Stielstra. 2012. "Changes in Snowpack Accumulation and Ablation in the Intermountain West." *Water Resources Research* 48 (11). https://doi.org/10.1029/2012WR011949.

Hejazi, M., J. Edmonds, L. Clarke, P. Kyle, E. Davies, V. Chaturvedi, M. Wise, P. Patel, J. Eom, and K. Calvin. 2014. "Long-Term Global Water Projections Using Six Socioeconomic Scenarios in an Integrated Assessment Modeling Framework." *Technological Forecasting and Social Change* 81: 205–26. https://doi.org/10.1016/j.techfore.2013.05.006.

Hodgkins, G.A., and R.W. Dudley. 2006. "Changes in the Timing of Winter–Spring Streamflows in Eastern North America, 1913–2002." *Geophysical Research Letters* 33 (6): 1913–2002. https://doi.org/10.1029/2005GL025593.

Issaka, S., and M.A. Ashraf. 2017. "Impact of Soil Erosion and Degradation on Water Quality: A Review." *Geology, Ecology, and Landscapes* 1 (1): 1–11. https://doi.org/10.1080/24749508.2017.1301053.

Kalin, L., and M.H. Hantush. 2006. "Comparative Assessment of Two Distributed Watershed Models with Application to a Small Watershed." *Hydrological processes* 20 (11): 2285–307. https://doi.org/10.1002/hyp.6063.

Kapnick, S., and A. Hall. 2012. "Causes of Recent Changes in Western North American Snowpack." *Climate Dynamics* 38 (9–10): 1885–99. https://doi.org/10.1007/s00382-011-1089-y.

Kaushal, S.S., P.M. Mayer, P.G. Vidon, R.M. Smith, M.J. Pennino, T.A. Newcomer, S. Duan, C. Welty, and K.T. Belt. 2014. "Land Use and Climate Variability Amplify Carbon, Nutrient, and Contaminant Pulses: A Review with Management Implications."

Journal of the American Water Resources Association 50 (3): 585–614. https://doi.org/10.1111/jawr.12204.

Kharel, G., H. Zheng, and A. Kirilenko. 2016. "Can Land-Use Change Mitigate Long-Term Flood Risks in the Prairie Pothole Region? The Case of Devils Lake, North Dakota, USA." *Regional Environmental Change* 16 (8): 2443–56. https://doi.org/10.1007/s10113-016-0970-y.

Khatri, K.B. 2013. *Risk and Uncertainty Analysis for Sustainable Urban Water Systems*. Leiden: CRC Press.

Khatri, K.B., C. Strong, A.K. Kochanski, S. Burian, C. Miller, and C. Hasenyager. 2018. "Water Resources Criticality Due to Future Climate Change and Population Growth: Case of River Basins in Utah, USA." *Journal of Water Resources Planning and Management* 144 (8): 04018041. https://doi.org/10.1061/(ASCE)WR.1943-5452.0000959.

Mahat, V., and D.G. Tarboton. 2012. "Canopy Radiation Transmission for an Energy Balance Snowmelt Model." *Water Resources Research* 48 (1). https://doi.org/10.1029/2011WR010438.

McCabe, G.J., and M.P. Clark. 2005. "Trends and Variability in Snowmelt Runoff in the Western United States." *Journal of Hydrometeorology* 6 (4): 476–82. https://doi.org/10.1175/JHM428.1.

Moore, J.N., J.T. Harper, and M.C. Greenwood. 2007. "Significance of Trends Toward Earlier Snowmelt Runoff, Columbia and Missouri Basin Headwaters, Western United States." *Geophysical Research Letters* 34 (16). https://doi.org/10.1029/2007GL031022.

Moore, L.W., H. Matheny, T. Tyree, D. Sabatini, and S.J. Klaine. 1988. "Agricultural Runoff Modeling in a Small West Tennessee watershed." *Journal (Water Pollution Control Federation)* 242–49. https://www.jstor.org/stable/25043487.

Moriasi, D.N., J.G. Arnold, M.W. Van Liew, R.L. Bingner, R.D. Harmel, and T.L. Veith. 2007. "Model Evaluation Guidelines for Systematic Quantification of Accuracy in Watershed Simulations." *Transactions of the American Society of Agricultural and Biological Engineers* 50 (3): 885–900. https://doi.org/10.13031/2013.23153.

Moss, R.H., J.A. Edmonds, K.A. Hibbard, M.R. Manning, S.K. Rose, D.P. Van Vuuren, T.R. Carter, S. Emori, M. Kainuma, and T. Kram. 2010. "The Next Generation of Scenarios for Climate Change Research and Assessment." *Nature* 463 (7282): 747. https://doi.org/10.1038/nature08823.

Mote, P.W., A.F. Hamlet, M.P. Clark, and D.P. Lettenmaier. 2005. "Declining Mountain Snowpack in Western North America." *Bulletin of the American Meteorological Society* 86 (1): 39–49. https://doi.org/10.1175/BAMS-86-1-39.

Mote, P.W., S. Li, D.P. Lettenmaier, M. Xiao, and R. Engel. 2018. "Dramatic Declines in Snowpack in the Western US." *Npj Climate and Atmospheric Science* 1 (1): 2. https://doi.org/10.1002/2016GL069965.

Mullan, D. 2013. "Soil Erosion under the Impacts of Future Climate Change: Assessing the Statistical Significance of Future Changes and the Potential On-Site and Off-Site Problems." *Catena* 109: 234–46. https://doi.org/10.1016/j.catena.2013.03.007.

Nunes, J., J. Seixas, and J. Keizer. 2013. "Modeling the Response of within-Storm Runoff and Erosion Dynamics to Climate Change in Two Mediterranean Watersheds: A Multi-Model, Multi-Scale Approach to Scenario Design and Analysis." *Catena* 102: 27–39. https://doi.org/10.1016/j.catena.2011.04.001.

Parsons, A.J., J. Wainwright, R.E. Brazier, and D.M. Powell. 2006. "Is Sediment Delivery a Fallacy?" *Earth Surface Processes and Landforms* 31 (10): 1325–28. https://doi.org/10.1002/esp.1395.

Pimentel, D., C. Wilson, C. McCullum, R. Huang, P. Dwen, J. Flack, Q. Tran, T. Saltman, and B. Cliff. 1997. "Economic and Environmental Benefits of Biodiversity." *BioScience* 47 (11): 747–57, https://www.jstor.org/stable/1313097.

Ray, A.J., J.J. Barsugli, K.B. Averyt, K. Wolter, M. Hoerling, N. Doesken, B. Udall, and R.S. Webb. 2008. "Climate Change in Colorado: A Synthesis to Support Water Resources Management and Adaptation." Colorado Water Conservation Board Rep.http://wwa.colorado.edu/climate/iwcs/archive/IWCS_2008_Nov_feature.pdf.

Reclamation. 2013. *Downscaled CMIP3 and CMIP5 Climate Projections: Release of Downscaled CMIP5 Climate Projections, Comparison with Preceding Information, and Summary of User Needs*. Denver, CO: U.S. Department of the Interior, Bureau of Reclamation, Technical Service Center. https://gdo-dcp.ucllnl.org/downscaled_cmip_projections/techmemo/downscaled_climate.pdf

Renard, K., D. Yoder, D. Lightle, and S. Dabney. 2011. "Universal Soil Loss Equation and Revised Universal Soil Loss Equation." *Handbook of Erosion Modeling* 8: 137–67. http://www.tucson.ars.ag.gov/unit/publications/pdffiles/2122.pdf.

Routschek, A., J. Schmidt, W. Enke, and T. Deutschlaender. 2014. "Future Soil Erosion Risk—Results of GIS-Based Model Simulations for a Catchment in Saxony/Germany." *Geomorphology* 206: 299–306. https://doi.org/10.1016/j.geomorph.2013.09.033.

Russell, M.J., D.E. Weller, T.E. Jordan, K.J. Sigwart, and K.J. Sullivan. 2008. "Net Anthropogenic Phosphorus Inputs: Spatial and Temporal Variability in the Chesapeake Bay Region." *Biogeochemistry* 88 (3): 285–304. https://doi.org/10.1007/s10533-008-9212-9.

Salt Lake County. 2017. "2015 Salt Lake County Integrated Watershed Plan, Update to the 2009 Salt Lake Countywide Water Quality Stewardship Plan Published September 2016 and Revised September 2017." https://slco.org/uploadedFiles/depot/publicWorks/fwatershed/resources/2015SLCoIWP.pdf.

Scalzitti, J., C. Strong, and A. Kochanski. 2016a. "Climate Change Impact on the Roles of Temperature and Precipitation in Western US snowpack Variability." *Geophysical Research Letters* 43 (10): 5361–69. https://doi.org/10.1002/2016GL068798.

Scalzitti, J., C. Strong, and A.K. Kochanski. 2016b. "A 26-Year High-Resolution Dynamical Downscaling over the Wasatch Mountains: Synoptic Effects on Winter Precipitation Performance." *Journal of Geophysical Research: Atmospheres* 121 (7): 3224–40. https://doi.org/10.1002/2015JD024497.

Simonovic, S.P. 2017. "Bringing Future Climatic Change into Water Resources Management Practice Today." *Water Resources Management* 31 (10): 2933–50. https://doi.org/10.1007/s11269-017-1704-8.

Skamarock, W.C., J.B. Klemp, J. Dudhia, D.O. Gill, D.M. Barker, W. Wang, and J.G. Powers. 2005. *A Description of the Advanced Research WRF Version 2*. Boulder, Co: National Center For Atmospheric Research and Mesoscale and Microscale Meteorology Division. http://citeseerx.ist.psu.edu/viewdoc/download?doi=10.1.1.484.3656&rep=rep1&type=pdf.

Smith, K., C. Strong, and S.-Y. Wang. 2015. "Connectivity between Historical Great Basin Precipitation and Pacific Ocean Variability: A CMIP5 Model Evaluation." *Journal of climate* 28 (15): 6096–112. https://doi.org/10.1175/JCLI-D-14-00488.1.

Stantec Consulting Inc. 2011. "Salt Lake Countywide Watershed Model Documentation." Prepared for Salt Lake County Public Works Department Engineering and Flood Control Division, Salt Lake County. https://deq.utah.gov/water-quality/watershed-monitoring-program/jordan-river-dissolved-oxygen-tmdl-watershed-management-program.

Stewart, I.T., D.R. Cayan, and M.D. Dettinger. 2005. "Changes Toward Earlier Streamflow Timing across Western North America." *Journal of climate* 18 (8): 1136–55. https://doi.org/10.1175/JCLI3321.1.

Strong, C., K.B. Khatri, A.K. Kochanski, C.S. Lewis, and L.N. Allen. 2017. "Reference Evapotranspiration from Coarse-Scale and Dynamically Downscaled Data in Complex Terrain: Sensitivity to Interpolation and Resolution." *Journal of Hydrology* 548: 406–18. https://doi.org/10.1016/j.jhydrol.2017.02.045.

Strong, C., A. Kochanski, and E. Crosman. 2014. "A Slab Model of the Great Salt Lake for Regional Climate Simulation." *Journal of Advances in Modeling Earth Systems* 6 (3): 602–15. https://doi.org/10.1002/2014MS000305.

Tasdighi, A., M. Arabi, and D.L. Osmond. 2017. "The Relationship between Land Use and Vulnerability to Nitrogen and Phosphorus Pollution in an Urban Watershed." *Journal of Environmental Quality* 46 (1): 113–22. https://doi.org/10.2134/jeq2016.06.0239.

Taylor, K.E., R.J. Stouffer, and G.A. Meehl. 2012. "An Overview of CMIP5 and the Experiment Design." *Bulletin of the American Meteorological Society* 93 (4): 485–98. https://doi.org/10.1175/BAMS-D-11-00094.1.

Tong, S.T., and W. Chen. 2002. "Modeling the Relationship between Land Use and Surface Water Quality." *Journal of Environmental Management* 66 (4): 377–93. https://doi.org/10.1006/jema.2002.0593.

USEPA (U.S. Environmental Protection Agency). 2007. *BASINS 4.0*. Washington, D.C.: U.S. Environmental Protection Agency. EPA-823-C-07-001. https://www.epa.gov/ceam/basins-download-and-installation.

Utah Governor's Office of Management and Budget. 2012. "2012 Baseline Projections." https://gomb.utah.gov/budget-policy/demographic-economic-analysis/.

Van Vuuren, D.P., J. Edmonds, M. Kainuma, K. Riahi, A. Thomson, K. Hibbard, G.C. Hurtt, T. Kram, V. Krey, and J.-F. Lamarque. 2011. "The Representative Concentration Pathways: An Overview." *Climatic Change* 109 (1–2): 5. https://doi.org/10.1007/s10584-011-0148-z.

Waddell, P. 2011. "Integrated Land Use and Transportation Planning and Modeling: Addressing Challenges in Research and Practice." *Transport Reviews* 31 (2): 209–29. https://doi.org/10.1080/01441647.2010.525671.

Wang, J.J., X. Lu, and M. Kummu. 2011. "Sediment Load Estimates and Variations in the Lower Mekong River." *River Research and Applications* 27 (1): 33–46. https://doi.org/10.1002/rra.1337.

Wasatch Front Regional Council. 2010. "The Greater Wasatch Vision for 2040." Salt Lake City.http://wasatchchoice2040.com/images/wc2040/FinalPoster_TheWasatchChoice2040_20Dec2010_Update_Reduced-2.pdf.

Wasatch Front Regional Council. 2015. "Regional Transportation Plan 2015–2040." *Salt Lake City*. http://www.wfrc.org/publications/RTP-publications/RTP_2015_FINAL.pdf.

Wilkinson, B.H., and B.J. McElroy. 2007. "The Impact of Humans on Continental Erosion and Sedimentation." *Geological Society of America Bulletin* 119 (1–2): 140–56. https://doi.org/10.1130/B25899.1.

Williams, R.E., M. Arabi, J. Loftis, and G.K. Elmund. 2014. "Monitoring Design for Assessing Compliance with Numeric Nutrient Standards for Rivers and Streams Using Geospatial Variables." *Journal of Environmental Quality* 43 (5): 1713–24.

Wurtsbaugh, W., C. Miller, S. Null, P. Wilcock, M. Hahnenberger, and F. Howe. 2016. "Impacts of Water Development on Great Salt Lake and the Wasatch Front." https://digitalcommons.usu.edu/wats_facpub/875.

Zahmatkesh, Z., M. Karamouz, E. Goharian, and S.J. Burian. 2014. "Analysis of the Effects of Climate Change on Urban Storm Water Runoff Using Statistically Downscaled Precipitation Data and a Change Factor Approach." *Journal of Hydrologic Engineering* 20 (7): 05014022. https://doi.org/10.1061/(ASCE)HE.1943-5584.0001064.

Zeckoski, R.W., M.D. Smolen, D.N. Moriasi, J.R. Frankenberger, and G.W. Feyereisen. 2015. "Hydrologic and Water Quality Terminology as Applied to Modeling." *Transactions of the American Society of Agricultural and Biological Engineers* 58 (6): 1619–35. https://doi.org/10.13031/trans.58.10713.